Development/Plasticity/Repair

Regional Specificity of GABAergic Regulation of Cross-Modal Plasticity in Mouse Visual Cortex after Unilateral Enucleation

Julie Nys, Katrien Smolders, Marie-Eve Laramée, Isabel Hofman, Tjing-Tjing Hu, and Lutgarde Arckens
Laboratory of Neuroplasticity and Neuroproteomics, KU Leuven, 3000 Leuven, Belgium

In adult mice, monocular enucleation (ME) results in an immediate deactivation of the contralateral medial monocular visual cortex. An early restricted reactivation by open eye potentiation is followed by a late overt cross-modal reactivation by whiskers (Van Brussel et al., 2011). In adolescence (P45), extensive recovery of cortical activity after ME fails as a result of suppression or functional immaturity of the cross-modal mechanisms (Nys et al., 2014). Here, we show that dark exposure before ME in adulthood also prevents the late cross-modal reactivation component, thereby converting the outcome of long-term ME into a more P45-like response. Because dark exposure affects GABAergic synaptic transmission in binocular V1 and the plastic immunity observed at P45 is reminiscent of the refractory period for inhibitory plasticity reported by Huang et al. (2010), we molecularly examined whether GABAergic inhibition also regulates ME-induced cross-modal plasticity. Comparison of the adaptation of the medial monocular and binocular cortices to long-term ME or dark exposure or a combinatorial deprivation revealed striking differences. In the medial monocular cortex, cortical inhibition via the $GABA_A$ receptor $\alpha 1$ subunit restricts cross-modal plasticity in P45 mice but is relaxed in adults to allow the whisker-mediated reactivation. In line, *in vivo* pharmacological activation of $\alpha 1$ subunit-containing $GABA_A$ receptors in adult ME mice specifically reduces the cross-modal aspect of reactivation. Together with region-specific changes in glutamate acid decarboxylase (GAD) and vesicular GABA transporter expression, these findings put intracortical inhibition forward as an important regulator of the age-, experience-, and cortical region-dependent cross-modal response to unilateral visual deprivation.

Key words: adulthood; cortical plasticity; dark exposure; $GABA_A$ receptor; *in situ* hybridization; multimodal

Significance Statement

In adult mice, vision loss through one eye instantly reduces neuronal activity in the visual cortex. Strengthening of remaining eye inputs in the binocular cortex is followed by cross-modal adaptations in the monocular cortex, in which whiskers become a dominant nonvisual input source to attain extensive cortical reactivation. We show that the cross-modal component does not occur in adolescence because of increased intracortical inhibition, a phenotype that was mimicked in adult enucleated mice when treated with indiplon, a $GABA_A$ receptor $\alpha 1$ agonist. The cross-modal versus unimodal responses of the adult monocular and binocular cortices also mirror regional specificity in inhibitory alterations after visual deprivation. Understanding cross-modal plasticity in response to sensory loss is essential to maximize patient susceptibility to sensory prosthetics.

Introduction

Monocular deprivation (MD) by eyelid suture is a popular paradigm to study structural and functional plasticity in the visual cortex of mammals (Morishita and Hensch, 2008). Monocular enucleation (ME) is a more complete deprivation strategy, excluding any remaining effect of spontaneous retinal activity (Nys

Received Sept. 11, 2014; revised June 3, 2015; accepted June 4, 2015.

Author contributions: J.N., T.-T.H., and L.A. designed research; J.N. and I.H. performed research; K.S., M.-E.L., I.H., and L.A. contributed unpublished reagents/analytic tools; J.N., K.S., I.H., T.-T.H., and L.A. analyzed data; J.N., M.-E.L., and L.A. wrote the paper.

This work was supported by Research Council of the KU Leuven Grant OT09/22 and the Fund for Scientific Research (FWO)-Flanders. J.N. is supported by a PhD grant from FWO-Flanders and Katrien Smolders by a PhD fellowship of the Agency for Innovation through Science and Technology Flanders (Innovation by Science and Technology (IWT) Vlaanderen). Marie-Eve Laramée is supported by a Fonds de la recherche en santé du Québec postdoctoral fellowship. We gratefully thank Ria Vanlaer and Lieve Geenen for excellent technical assistance and Denis Boire (Trois-Rivières University of Quebec, Quebec, Canada) for his critical input. We also thank Zsuzsanna Vegh (KU Leuven, Leuven, Belgium) for her practical assistance in the locomotion experiments and Jean-Pierre Sommeijer (Netherlands Institute for Neuroscience, Amsterdam, The Netherlands) for providing helpful advice on indiplon administration.

The authors declare no competing financial interest.

Correspondence should be addressed to Dr. Lutgarde Arckens, Laboratory of Neuroplasticity and Neuroproteomics, KU Leuven, Naamsestraat 59, Box 2467, B-3000 Leuven, Belgium. E-mail: Lut.Arckens@bio.kuleuven.be.

DOI:10.1523/JNEUROSCI.3808-14.2015

 0270-6474/15/3511174-16$15.00/0

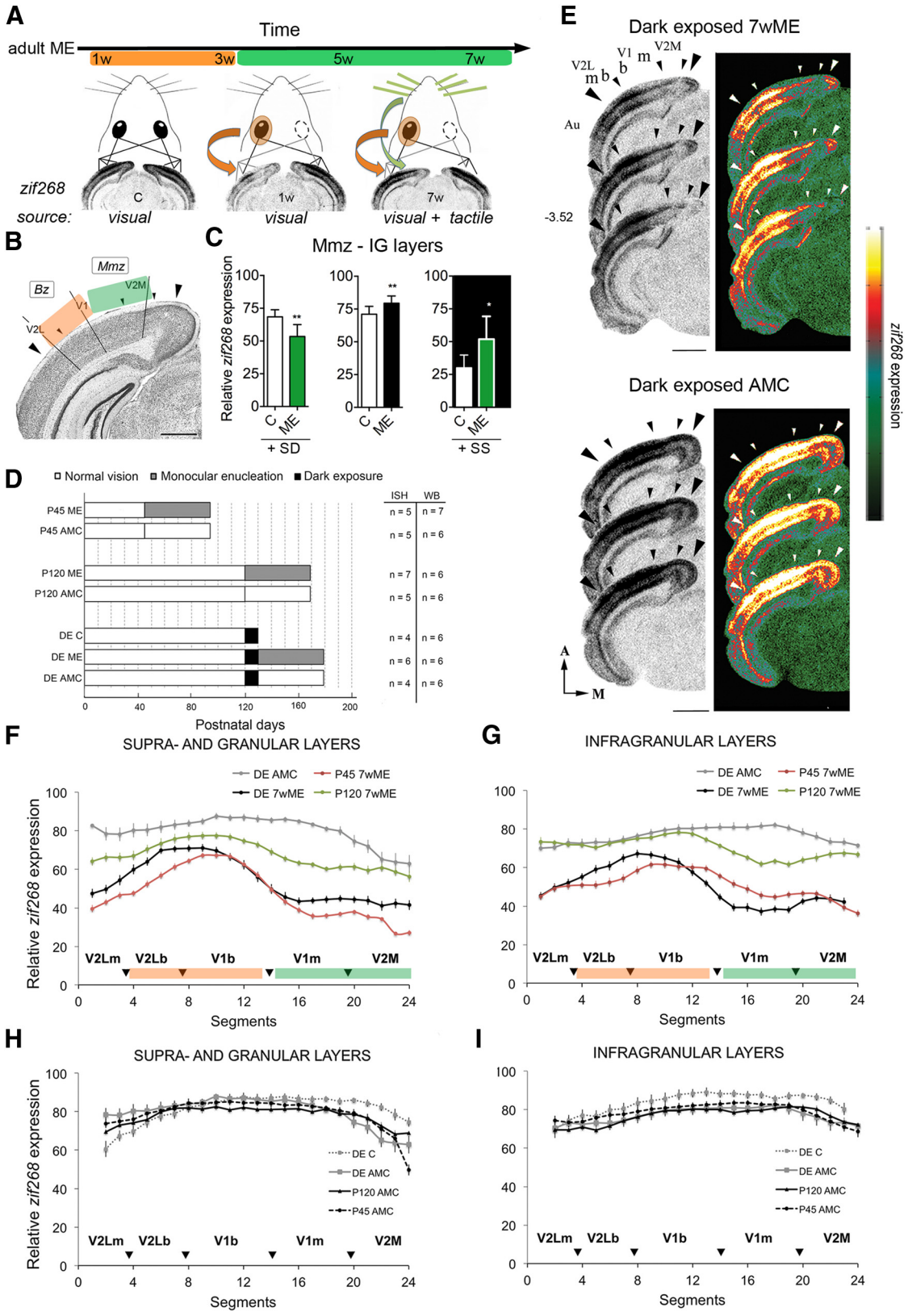

Figure 1. DE before ME in adulthood induces an adolescent P45-like visual cortex reactivation pattern after 7 weeks of ME. ***A***, Schematic representation of the early open eye potentiation phase (orange; weeks 1–3) and the late cross-modal phase (green; weeks 3–7) of cortical plasticity in response to ME as measured by cortical region- and time-specific *zif268* expression (based on the study by Van Brussel et al., 2011). The visual/tactile origin of *zif268* induction is indicated below the pictograms and ISH autoradiograms for control, 1 week (1w) ME, and 7 week (7w) ME mice. ***B***, Nissl-stained coronal section of the mouse visual cortex. Scale bar, 1 mm. Large arrowheads demarcate the mediolateral extent of the visual cortex; small arrowheads indicate interareal boundaries. The functional subdivisions of interest: Mmz and Bz are depicted in green and orange, respectively, consistent with the dominant type of plasticity and input source after long-term ME. ***C***, Whisker trimming and stimulation (green) in 7wME mice as proof of the tactile origin of *zif268* induction in the Mmz after long-term ME. Quantitative data from the infragranular layers are shown as examples. SD by trimming the right-side vibrissae decreases neuronal activity, whereas SS via exposure to toys and novel objects in the dark increases (*Figure legend continues.*)

et al., 2015). Both deprivation strategies delivered solid proof for ocular dominance plasticity in the binocular cortex (Tagawa et al., 2005; Syken et al., 2006; Datwani et al., 2009; Kanold et al., 2009). ME additionally leads to cross-modal adaptations in monocular and extrastriate (V2) areas in the rat (Toldi et al., 1994, 1996; Hada et al., 1999; Yagi et al., 2001). The concerted action of these two plasticity phenomena also restores neuronal activity throughout the contralateral visual cortex of adult ME mice. After ME, open eye input mediates an initial partial reactivation of the monocular portion of the visual cortex devoted previously to the removed eye. Several weeks after ME, once reactivation is completed, whisker trimming and stimulation uncovered a clear tactile activation of the medial monocular cortex in adult long-term ME mice (Van Brussel et al., 2011; Fig. 1*A–C*). In contrast, when ME is induced at P45, the plasticity response remains primarily confined to the early visually driven reactivation (Nys et al., 2014), reminiscent of the constraint on experience-induced inhibitory plasticity in adolescent rats reported by Huang et al. (2010).

To date, little is known about the molecular switches for cross-modal plasticity in the sensory neocortex. GABAergic inhibition is a potential candidate. It adapts to altered sensory experience (Pallas, 2001; Desgent et al., 2010; Wenner, 2011), and it tightly regulates the activity of cortico-(thalamo-)cortical inputs (Callaway, 2004; Petrus et al. 2014) and, as such, is capable of controlling the expression of diverse types of neuronal plasticity. Also, cortical inhibition has been suggested to be involved in multisensory integration (Meredith, 2002; Friedel and Hemmen, 2008; Olcese et al., 2013; Gogolla et al., 2014). In the binocular cortex of adult rats, dark exposure (DE) acutely influences the level of GABAergic transmission, thereby reinstating robust ocular dominance plasticity in response to short-term MD (He et al., 2006, 2007; Huang et al., 2010). If DE also influences the local GABA ergic circuitry in the mouse monocular cortex, this could possibly act as an off switch for cross-modal plasticity in adulthood as a return to a cortical P45 status.

To test whether intracortical inhibition exerts such a prominent role in the distinct age- and experience-dependent reactivation of the medial monocular and binocular cortices after ME, we performed two types of experiments. First, we compared the recovery of neuronal activity over the full extent of the visual cortex of three groups of long-term enucleated mice: (1) dark-exposed adults; (2) normally reared adults; and (3) P45 animals. Cortical *zif268* expression patterns were used as a readout for experience-induced neuronal activity. In parallel, we performed Western blot analysis separately for monocular and binocular cortices for a set of presynaptic and postsynaptic inhibitory markers, next to *in vivo* pharmacological manipulation of $GABA_A$ receptors.

Materials and Methods

Animals

C57BL/6J mice ($n = 78$) of either sex were housed under standard laboratory conditions under an 11/13 h dark/light cycle with food and water available *ad libitum*. All experiments were approved by the ethical committee of KU Leuven and were in strict accordance with the European Communities Council Directive of September 22, 2010 (2010/63/EU) and with Belgian legislation (Royal Decree of May 29, 2013). Every possible effort was made to minimize animal suffering and to reduce the number of animals.

Visual deprivation paradigms and tissue preparation

Independent of visual manipulation, all mice were kept in a natural environment in relation to auditory and somatosensory stimulation.

Dark exposure. Dark-exposed mice refer to adult mice that were normally reared until the age of P120, when they were then moved into a light-tight dark room for a subsequent visual deprivation period of 10 d, a duration that is in accordance with the studies by He et al. (2006), He et al. (2007), and Huang et al. (2010). During this period, they were checked regularly under limited visible red light.

Monocular enucleation. Figure 1*D* illustrates the different experimental conditions used in this study. We analyzed the brains of C57BL/6J mice of different ages (P45 and P120), different visual experience histories (DE or not, in black), and enucleated or not (gray vs white). The 7 week enucleated (7wME) subjects were always compared with non-deprived age-matched controls (AMCs) to allow a correct interpretation of the data as a specific result of ME, so all bar graphs in Figures 2–4 depict a ratio of 7wME/AMC in which the neuronal activity levels (*zif268* expression) or protein expression levels of each enucleated group were normalized to their AMCs. In relation to the DE pretreatment, an additional control (DE C) was included consisting of mice killed immediately after DE to discriminate between the effects of DE alone or DE in combination with ME on cortical activity and protein expression levels in P120 mice.

The removal of the right eye, or ME, of the mice was performed as described previously (Aerts et al., 2014; Nys et al., 2014). Briefly, under anesthesia by intraperitoneal injection of a mixture of ketamine hydrochloride (75 mg/kg; Eurovet; Dechra Veterinary Products) and medetomidine hydrochloride (1 mg/kg; Orion; Janssen), the right eye was removed carefully, and the orbit was filled with hemostatic cotton wool (Qualiphar). After injection with atipamezol hydrochloride (1 mg/kg; Orion; Elanco) to reverse anesthesia, the animals were allowed to recover on a heating pad. They were all administered meloxicam (1 mg/kg; Boehringer Ingelheim) intraperitoneally every 24 h in the next days as a systemic analgesic. After the enucleation procedure, mice were again housed in standard cages under the same normal lighting conditions for the required survival period. Intact control animals were also maintained in the similar housing and light environment.

All mice received an overdose of sodium pentobarbital (Nembutal, 600 mg/kg; Ceva Santa Animale) by intraperitoneal injection before they were killed by cervical dislocation. The brains were removed rapidly and frozen immediately in 2-methylbutane (Merck) at a temperature of −40°C and stored at −80°C until sectioning. For *in situ* hybridization (ISH) experiments, 25-μm-thick sections were prepared on a cryostat (HM 500 OM; Microm), mounted on 0.1% poly-L-lysine-coated (Sigma-Aldrich) slides, and stored at −20°C until additional processing. For Western blotting (WB), 100-μm-thick coronal cryosections were collected on baked slides and stored at −80°C.

In situ *hybridization for* zif268

We performed radioactive ISH experiments (Fig. 1*D*; ISH, $n = 36$) on series of coronal brain sections between bregma −1.82 and −4.36 mm to examine the spatial extent and the exact anatomical location of

←

(*Figure legend continued.*) relative *zif268* expression (adapted from Van Brussel et al., 2011). ***D***, Schematic representation of the experimental setup used in this study. Three groups representing adolescence (P45), adulthood (P120), and an additional group subjected to 10 d of total darkness starting at P120 and before ME (DE; black bars) were analyzed and compared. Different subgroups included the following: (1) a 7wME group (gray bars) with the right eye enucleated; (2) a control group representing a nondeprived AMC (white bars); and (3) a specific dark-exposed control group (DE C). The numbers of animals (*n*) used in the ISH and WB experiments are indicated next to each bar. ***E***, Images of three adjacent sections around bregma level −3.52 mm from dark-exposed enucleated (DE 7wME) and dark-exposed AMC mice (DE AMC). The corresponding pseudocolor representations of signal intensity differences are displayed next to each triplet of ISH sections. Scale bars, 2 mm. ***F***, ***G***, The line graphs illustrate the relative *zif268* expression for the upper (II–IV) and lower (V–VI) layers along the five predefined visual subdivisions (black arrowheads are in correspondence with the small arrowheads in the images in ***E***) measured as the average OD in each segment for DE AMC (gray), DE 7wME (black) next to P45 7wME (red) and P120 7wME (green) animals (Nys et al. 2014). Error bars represent the SEM of the mean OD in each segment. ***H***, ***I***, Comparison of *zif268* expression levels in the left visual cortex of four control groups: (1) P120 AMC (black); (2) P45 AMC (stippled black); (3) DE AMC (gray); and (4) DE C (stippled gray). A, Anterior; M, medial; m, monocular; b, binocular; IG, infragranular layers.

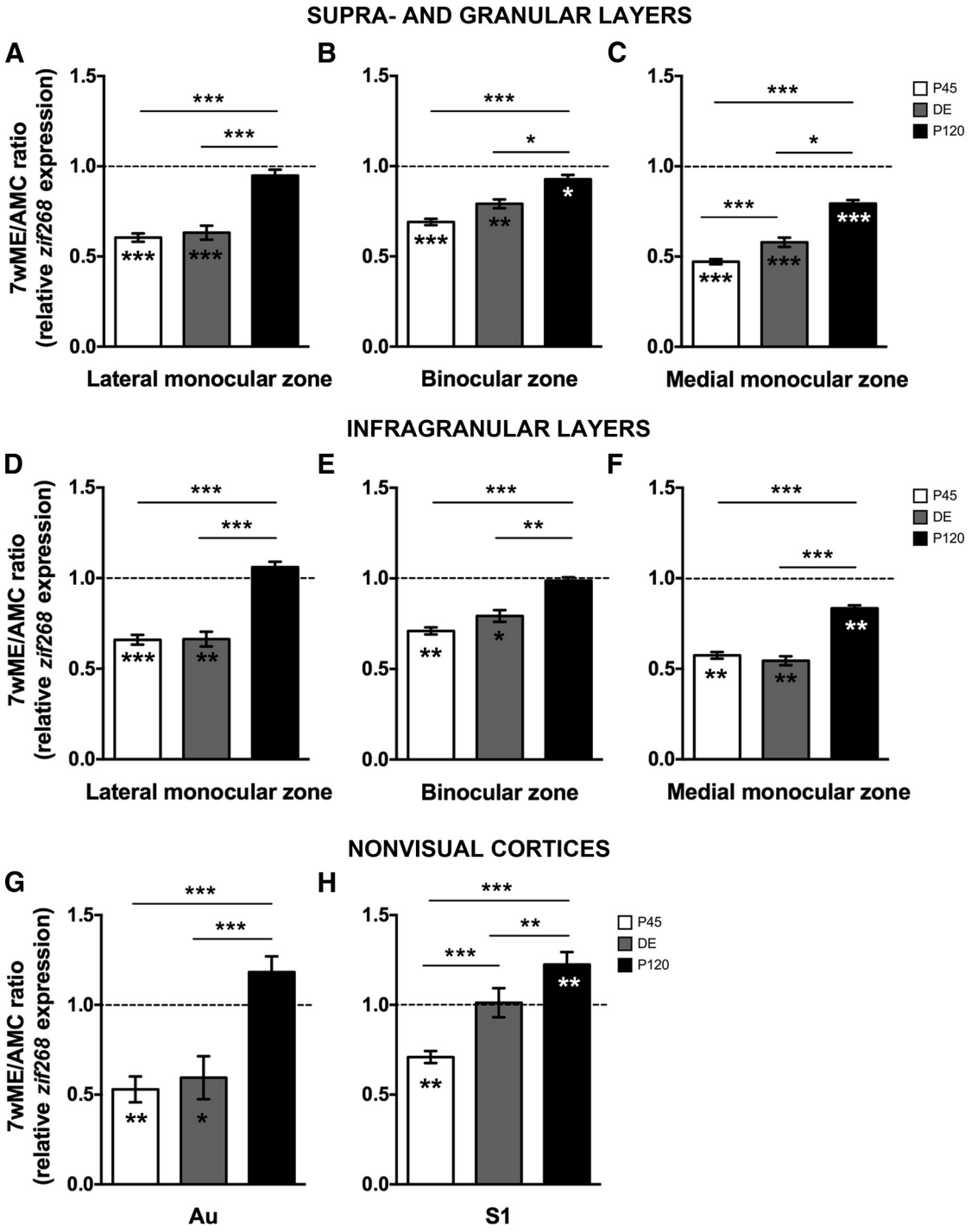

Figure 2. The effect of DE on *zif268*-based activity levels in visual and nonvisual cortices after 7 weeks of ME. ***A–F***, DE in adulthood rejuvenates the ME-induced activity along the different functional subdivisions and cortical layers of the deprived visual cortex. Normalized subdivision-specific ODs for P45 (white), DE (gray), and P120 (black) 7wME mice are shown by dividing the relative *zif268* expression of each ME group to its AMC level (7wME/AMC ratio). A direct comparison of ME-induced reactivation levels as a function of age and dark treatment confirmed a limited reactivation pattern, similar to P45, across the upper and lower layers in dark-exposed adult mice. Error bars represent the SEM. ***G***, ***H***, DE also reduced the neuronal activity across all layers of nonvisual areas compared with normally reared adults after 7 weeks of ME. Normalized ODs for P45 (white), DE (gray), and P120 (black) 7wME mice are shown for auditory (***G***) and somatosensory (***H***) cortices. In contrast to P120, the auditory cortex of DE 7wME mice (average ± SEM, 36.65 ± 4.62) showed a hypoactive state compared with DE AMC mice (61.66 ± 6.67), which closely resembles P45 7wME. In the somatosensory cortex, DE triggered intermediate activity levels (DE 7wME mice, 60.28 ± 2.61; DE AMC mice, 59.56 ± 4.00) compared with P120 and P45 7wME.

experience-induced neuronal activity changes throughout the sensory neocortex of mice from all experimental conditions. This was achieved by measuring the changes in the expression of the immediate early gene (IEG) *zif268*, a proven excellent activity reporter gene in the mammalian brain (mouse: Van Brussel et al., 2009, 2011; Woolley et al., 2013; Imbrosci et al., 2014; Nys et al., 2014; cat: Arckens et al., 2000b; Qu et al., 2003; Massie et al., 2003a,3b; Leysen et al., 2004). Preferential expression of Zif268 protein in excitatory neurons has been demonstrated elegantly in the monkey visual cortex (Chaudhuri et al., 1995; Kaczmarek and Chaudhuri, 1997). Combined with the notion that *zif268* expression can be tightly regulated by pharmacologically manipulating excitatory transmission (Saffen et al., 1988; Cole et al., 1989; Worley et al., 1991; Mataga

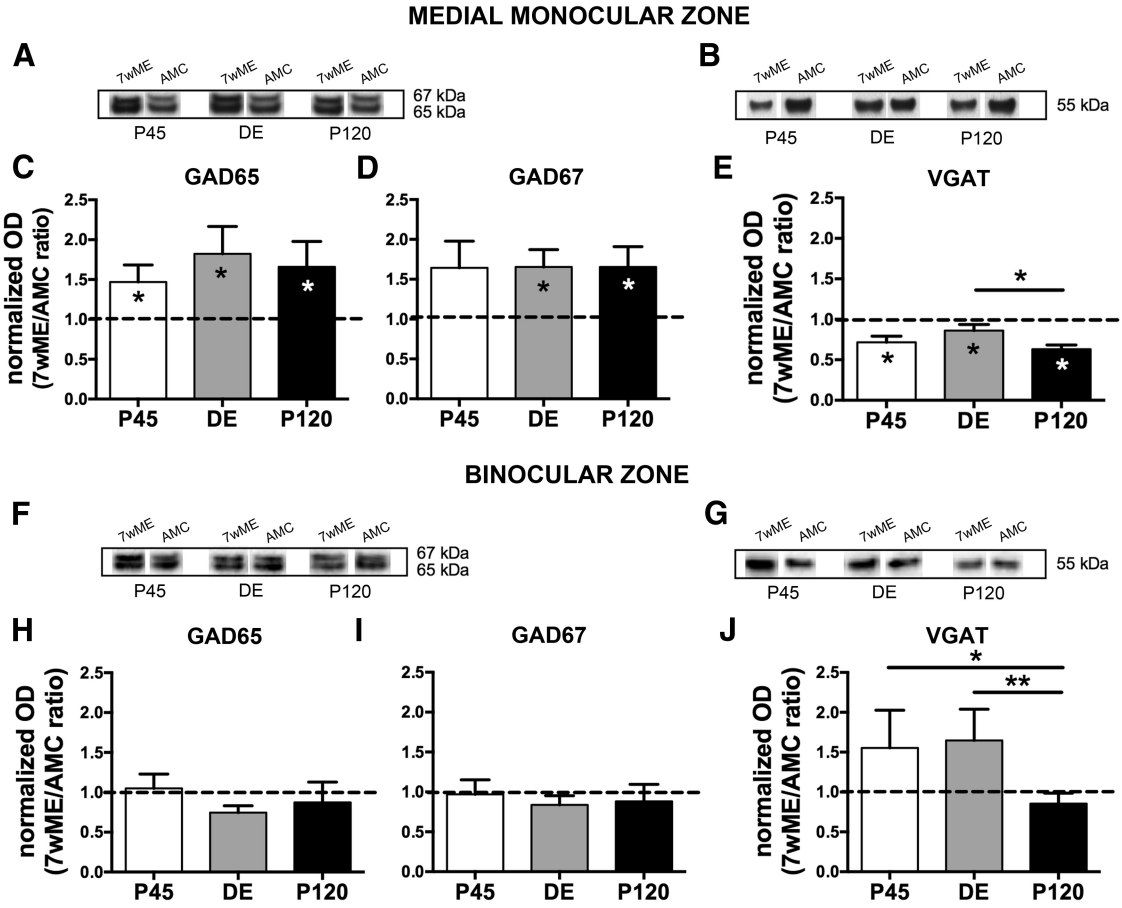

Figure 3. Long-term ME induced different expression changes of presynaptic inhibitory markers in the contralateral medial monocular and binocular cortices. Representative Western blot bands from functional subdivision-specific homogenates and their molecular weight are shown above the bar graphs for GAD65, GAD67 (***A***, ***F***), and VGAT (***B***, ***G***) proteins. ODs of WB results are illustrated as the 7wME expression levels normalized relative to the expression of its corresponding AMC group (7wME/AMC ratio) to allow a direct comparison of protein levels between the different ME groups of P45 (white), DE (gray), and P120 (black) mice. In the medial monocular cortex (***A–E***) of all experimental groups, a significant increase of GAD65 (***C***; average 7wME ± SEM, P45, 1.40 ± 0.15; DE, 1.75 ± 0.27; P120, 1.58 ± 0.23) and GAD67 (***D***; DE, 1.80 ± 0.29; P120, 1.63 ± 0.22; except P45, 1.67 ± 0.28) was observed 7 weeks after ME compared with AMC levels (***C***: average controls ± SEM, P45, 0.95 ± 0.09; DE, 0.96 ± 0.10; P120, 0.95 ± 0.12; ***D***: P45, 1.02 ± 0.11; DE, 1.09 ± 0.10; P120, 0.99 ± 0.14), whereas the expression of VGAT (***E***) of all P45, DE, and P120 7wME (average 7wME ± SEM, P45, 0.83 ± 0.07; DE, 0.72 ± 0.04; P120, 0.67 ± 0.05) mice was significantly reduced in relation to AMCs (average controls ± SEM, P45, 1.16 ± 0.06; DE, 0.83 ± 0.06; P120, 1.06 ± 0.02). In contrast, for the binocular cortex (***F–J***), no significant ME effect was found for GAD proteins (***H***: average 7wME ± SEM, P45, 1.42 ± 0.17; DE, 1.12 ± 0.12; P120, 1.04 ± 0.18; ***I***: P45, 1.38 ± 0.19; DE, 1.22 ± 0.13; P120, 1.12 ± 0.17) or VGAT (***J***; average 7wME ± SEM, P45, 1.36 ± 0.11; DE, 1.20 ± 0.20; P120, 0.70 ± 0.08) compared with their AMC (***H***: average controls ± SEM, P45, 1.35 ± 0.17; DE, 1.50 ± 0.07; P120, 1.19 ± 0.28; ***I***: P45, 1.42 ± 0.18; DE, 1.45 ± 0.08; P120, 1.27 ± 0.30; ***J***: P45, 0.88 ± 0.26; DE, 0.73 ± 0.12; P120, 0.82 ± 0.09). However, P45 and DE mice revealed a higher VGAT ratio compared with P120 mice.

et al., 2001), we interpret the ISH experiments for *zif268* as the predominant activation of cortical excitatory neurons.

ISH was performed with a mouse-specific synthetic oligonucleotide probe (Eurogentec) sequence (5′- ccgttgctcagcagcatcatctcctccagtttgggg gtagttgtcc-3′) for *zif268*. As described previously (Arckens et al., 1995; Nys et al., 2014), each probe was 3′ end labeled with [^{33}P]dATP using terminal deoxynucleotidyl transferase (Invitrogen). Unincorporated nucleotides were separated from the labeled probe with miniQuick Spin Oligo Columns (Roche Diagnostics). Series of cryostat sections for *zif268* were fixed, dehydrated, and delipidated. The radioactively labeled probe was added to a hybridization mixture [50% (v/v) formamide, 4× standard SSC buffer, 1× Denhardt's solution, 10% (w/v) dextran sulfate, 100 μg/ml herring sperm DNA, 250 μg/ml tRNA, 60 mM dithiothreitol, 1% (w/v) *N*-lauroyl sarcosine, and 20 mM $NaHPO_4$, pH 7.4] and applied to the cryostat sections (10^6 cpm/section) for an overnight incubation at 37°C in a humid chamber. The following day, sections were rinsed in 1× standard SSC buffer at a temperature of 42°C, dehydrated, air dried, and exposed to an autoradiographic film (Biomax MR; Kodak). Films for *zif268* were developed in Kodak D19 developing solution after 6 d. Fixation was performed in Rapid fixer (Ilford Hypam; Kodak).

For each mouse, autoradiographic images from three adjacent sections were scanned at 1200 dpi (CanoScan LIDE 600F; Canon), and all files were similarly adjusted for brightness and contrast in Adobe Photoshop CS5 (Adobe Systems). Pseudo-color maps (Fig. 1*E*) were generated with a custom-made MATLAB script (MATLAB R2008b; MathWorks) and represent a false coloring of the gray values: a high gray value is represented in white/yellow and a low gray value in black/green, indicating a low signal response or a high signal response, respectively. This is done in accordance with a grayscale ranging from black (0) to white (255).

Interpretation of the zif268 *expression levels*

The freely moving mice were always put in darkness overnight and then exposed to 45 min of bright light (always between 9:00 A.M. and 11:00 A.M. to minimize any possible variation attributable to time of the day; with exposure to normal everyday sounds and somatosensation) before they were killed. Importantly, such an overnight darkness period is not sufficient to elicit cross-modal plasticity (Goel et al., 2006, Goel and Lee, 2007; Jitsuki et al., 2011). In subjects in which cross-modal brain plasticity does not occur, i.e., controls and short-term ME mice, *zif268* expression therefore reflects the actual influence of visual stimulation on the visual cortex (Worley et al., 1991; Zhang et al., 1994; Kaczmarek and Chaudhuri, 1997; Arckens et al., 2000b; Zangenehpour and Chaudhuri, 2002; Van der Gucht et al., 2007). The cortical activity pattern of short-term (1 week) ME mice indeed clearly demonstrates still low IEG expres-

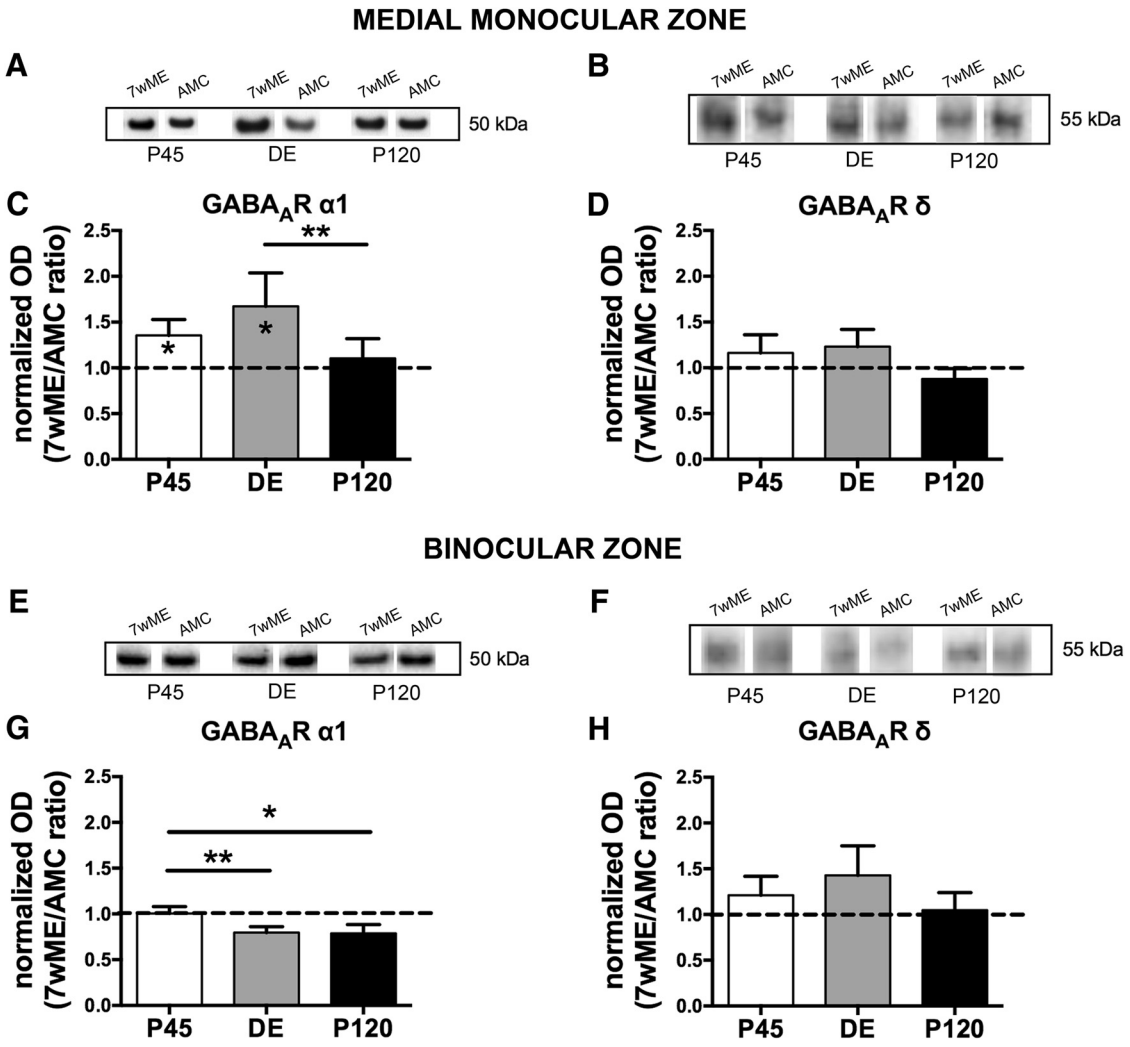

Figure 4. Long-term ME triggered distinct alterations in the protein expression of the $GABA_A$ receptor α1 but not the δ subunit in the contralateral medial monocular and binocular cortices. Representative Western blot bands from functional subdivision-specific homogenates and their molecular weight are shown above the functional subdivision-related bar graphs for the $GABA_A$ receptor α1 subunit (***A***, ***E***) and the $GABA_A$ receptor δ subunit (***B***, ***F***) proteins. In the medial monocular cortex (***A–D***) of both P45 and DE 7wME (average 7wME ± SEM, P45, 1.27 ± 0.10; DE, 1.27 ± 0.09; P120, 1.02 ± 0.11), the $GABA_A$ α1 subunit receptor (***C***) revealed a significant upregulation compared with AMC levels (average controls ± SEM, P45, 0.94 ± 0.10; DE, 0.76 ± 0.15; P120, 0.93 ± 0.03), whereas no significant changes in expression level were observed for the $GABA_A$ receptor δ subunit (***D***; average 7wME ± SEM, P45, 1.23 ± 0.16; DE, 0.99 ± 0.18; P120, 0.80 ± 0.09; average controls ± SEM, P45, 1.06 ± 0.11; DE, 0.82 ± 0.08; P120, 1.02 ± 0.13). The binocular cortex revealed no significant changes (***G***, ***H***) for either subunit of the $GABA_A$ receptor (***G***: average 7wME ± SEM, P45, 1.35 ± 0.05; DE, 1.08 ± 0.07; P120, 1.04 ± 0.06; average controls ± SEM, P45, 1.34 ± 0.09; DE, 1.36 ± 0.07; P120, 1.32 ± 0.14; ***H***: average 7wME ± SEM, P45, 1.34 ± 0.13; DE, 1.17 ± 0.18; P120, 1.00 ± 0.17; average controls ± SEM, P45, 1.11 ± 0.16; DE, 0.82 ± 0.14; P120, 0.95 ± 0.07).

sion levels in the contralateral deprived visual cortex, especially in the medial monocular cortical territory that is not driven by open eye input at this time (Fig. 1*A*; Van Brussel et al., 2011; Nys et al., 2014).

From several weeks after ME onward, whisking as a result of natural exploration behavior starts to drive *zif268* expression in the medial monocular cortex. Figure 1*A* illustrates how the initial open eye potentiation leads to the expansion of the binocular cortex into monocular territory (Fig. 1*A*, orange, *B*, Bz) and how nonvisual inputs take part in the next phase of recovery of neuronal activity (Fig. 1*A*, green, *B*, Mmz): natural whisking for 7 weeks in adult ME mice accounts for the strengthening of whisker-related inputs into visual areas to a level strong enough to drive high *zif268* expression, especially in the medial monocular cortex. Three previous observations (Van Brussel et al., 2011) support somatosensory activation of the visual cortex in ME mice: (1) somatosensory deprivation (SD) by unilateral whisker removal after long-term ME significantly decreases *zif268* expression in the medial monocular cortex (Fig. 1*C*, SD); (2) somatosensory stimulation (SS) by means of tactile exploration of toys in the dark (Fig. 1*C*, SS) results in increased *zif268* induction in the medial monocular cortex; and (3) enucleation of the remaining open eye has little effect on the *zif268* expression in the medial monocular cortex of adult 7wME mice. In summary, these observations rule out a purely visually driven *zif268* expression in 7wME mice as in control mice and additionally make it unlikely that putative higher-order feedback into monocular cortex, carrying binocular information, would be the origin of the re-gained neuronal activity. Consequently, the source of *zif268* induction in the visual cortex in our setup (Fig. 1*A*,*D*) strongly depends on the experimental condition (control/enucleated), the post-ME survival time (weeks), and the functional cortical region under study (Fig. 1*B*, Mmz/Bz) within the mouse visual cortex. For instance, in the full visual cortex of control mice (Fig. 1*A*, left) and in the binocular zone (Bz) of enucleated animals (Fig. 1*A*, middle), the *zif268* expression pattern primarily reflects visual experience-driven activity. In adult 7wME mice, particularly in the medial monocular cortex, it mainly reflects nonvisual whisker inputs (Fig. 1*A*,*C*, green; Van Brussel et al., 2011).

Histology

Histology was performed to aid interpretation of the activity patterns obtained by ISH. The cryostat sections for *zif268* were always Nissl counterstained (1% cresyl violet; Fluka, Sigma-Aldrich) according to standard procedures. Comparisons were made with the stereotaxic mouse brain

atlas (Franklin and Paxinos, 2008). Images of the stained coronal sections were obtained with a light microscope (Zeiss Axio Imager Z1) equipped with an AxioCam MRm camera (1388 × 1040 pixels) using the software program Axiovision release 4.6 (Carl Zeiss-Benelux).

Localization of visual areal boundaries with Nissl patterns

To delineate anatomically the areal borders of the different visual cortex subdivisions, a comparison was made with Nissl counterstained sections as described previously (Van Brussel et al., 2009; Nys et al., 2014). All topographic denominations were adopted from these studies (Fig. 1*B*). Concurrently, we applied the mapping of the monocular and binocular zones as functional subdivisions within the visual cortex as defined by Van Brussel et al. (2009). These methods allowed for the generation of animal-specific coronal atlases of the visual cortex and thus provided a reliable guide for the interpretation of *zif268* ISH results. In all figures, the large arrowheads indicate the total extent of the visual cortex, and small arrowheads indicate the areal borders. We always distinguished five subregions from medial to lateral: the medial extrastriate cortex (V2M), the primary visual cortex (V1), which we subdivided in the monocular (V1m) and binocular (V1b) parts, and the lateral extrastriate cortex (V2L), which was also subdivided in monocular (V2Lm) and binocular (V2Lb) regions (Van der Gucht et al., 2007; Van Brussel et al., 2009; Nys et al., 2014). In relation to functional inputs, we defined the cortical region encompassing the V1–V2L border as the Bz, a large part of V2M and V1m as the medial monocular zone (Mmz), and V2Lm as the lateral monocular zone (Lmz). In Figure 1*E*, the location of the Bz has been indicated with the small letter b, and the adjoining monocular driven parts of V1 and V2L are marked with a small letter m.

Quantitative analysis of ISH results

To quantify the optical density (OD; mean gray value per pixel) of the ISH autoradiograms, we used a custom-made MATLAB script (MATLAB R2008b; MathWorks) as described previously (Nys et al., 2014). For each condition, at least four mice (Fig. 1*D*) were included, and, for each mouse, three 25 μm sections were selected between −3.0 and −4.0 mm relative to bregma (Franklin and Paxinos, 2008), including visual and auditory [encompassing the dorsal secondary auditory cortex (AuD), the primary auditory cortex (Au1), and the ventral secondary auditory cortex (AuV)] cortices. Primary somatosensory cortex (S1) activity patterns were quantified on sections between −1.82 and −2.18 mm relative to bregma (Franklin and Paxinos, 2008). To demarcate the region of interest in the left hemisphere, we determined the top edge of the cortex, the border between the granular layer IV and infragranular layer V and the boundary at which layer VI meets the white matter. The delineated region of interest was divided equally into 24 segments to create two lattices of 24 quadrangles, corresponding to the upper (II–IV) and lower (V–VI) layers. To compensate for possible variation in brain size and morphology, we translated the lattice on each autoradiogram over the cortical curvature, fixing the border of a specific segment to an areal border (border segment 19/20 is the area border V1m/V2M). For each segment created this way, the relative OD was calculated as the mean gray value of all pixels within this quadrangle normalized to the mean gray value of a square measured in the thalamus (a defined region with no *zif268* expression above background). This procedure was required to compare autoradiograms across experiments (Paulussen et al., 2011; Van Brussel et al., 2011; Imbrosci et al., 2014; Nys et al., 2014). Relative neuronal activity was expressed in percentages based on the following formula: [1 − (cortical *zif268*/thalamic background)] × 100.

Western blot analysis

To visualize changes in the presence and relative amount of presynaptic and postsynaptic proteins involved in GABAergic signaling, we used WB. For each condition, at least six mice were included (Fig. 1*D*; WB, $n = 43$).

Protein extraction. The left medial monocular and binocular cortices were collected separately (Fig. 1*B*) from the 100-μm-thick coronal cryosections spanning bregma levels −2.0 to −4.60 mm and containing all layers. Proteins were extracted with a lysis buffer (65 mM Tris-HCl, 2% w/v SDS, and a mix of protease inhibitors; Roche) optimized for the enrichment of membrane (-associated) proteins (Wakabayashi et al., 1999; Van Damme et al., 2003). After mechanical homogenization by drill-driven pestles and sonication for five times for 10 s, the samples were heated at 70°C for 5 min and centrifuged for 15 min at 13,000 × *g* at 4°C. The supernatant was isolated, and the total protein concentration was determined according to the Qubit Quantitation Platform (Invitrogen) using a Qubit fluorometer (Invitrogen). Samples were kept at −80°C.

Immunoblotting. To obtain the optimal protein load, a protein dilution series ranging from 2.5 to 20 μg was analyzed. A concentration within the linear range of the detection system that resulted in a good signal-to-noise ratio was chosen for monocular and binocular samples separately. For glutamate acid decarboxylase (GAD) 65/67, this resulted in 15 μg for monocular samples and 5 μg for binocular samples. In the case of vesicular GABA transporter (VGAT) analysis, 7.5 μg for monocular and 10 μg for binocular samples were used. For the $GABA_A$ δ receptor subunit, 10 μg was used. For the $GABA_A$ receptor α1 subunit, the optimal protein load was 7.5 μg for all samples. A reference sample (pool) consisting of a mixture of each prepared tissue sample for monocular or binocular cortex was run with the same optimal amount of protein on each gel to gauge blot-to-blot variability. After the addition of 5 μl reducing agent (10×; Invitrogen) and 2 μl of lithium dodecyl sulfate sample buffer (4×; Invitrogen), the samples were denatured (10 min, 70°C). The protein samples were separated on 4–12% Bis-Tris Midi-gels in the XCell4 SureLock Midi-Cell (Invitrogen). Samples for each individual mouse were run in duplicate for each protein of interest, with monocular and binocular cortex samples run on different gels. The Spectra Multicolor High range protein ladder (Thermo Fisher Scientific) was used as molecular weight standard. Subsequently, the samples were transferred to a polyvinylidene fluoride or nitrocellulose (for VGAT and the $GABA_A$ δ receptor subunit) membrane (iBlot, Gel Transfer Stack; Invitrogen).

After 1–2 h incubation in a 5% ECL blocking agent (GE Healthcare) in Tris-saline (0.01 M Tris, 0.9% NaCl, and 0.1% Triton X-100, pH 7.6), the membrane was incubated overnight with a primary antibody raised in rabbit that recognizes both isoforms of GAD (GAD65 and GAD67; 1:6000; Abcam), with rabbit anti-VGAT (1:1000; Abcam), rabbit anti-$GABA_A$ receptor α1 subunit (1:1000; Alomone Labs), or mouse anti-$GABA_A$ receptor δ subunit (1:200; Neuromab). The next day, the blots were washed successively in Tris-saline (four times for 7 min), incubated for 30 min with HRP-conjugated secondary antibody (goat anti-rabbit and goat anti-mouse IgG; 1:50,000; Dako), rinsed in Tris-saline (five times for 7 min) and Tris-stock (one time for 5 min; 0.05 M Tris, pH 7.6), and incubated for 5 min in Super Signal West Dura (Pierce). The immunoreactive bands were visualized using a chemiluminescent reaction (Supersignal West Dura; Thermo Fisher Scientific, Pierce) combined with ECL hyperfilm (GE Healthcare) exposure or with the Bio-Rad Chemi-Doc MP Imaging System. To correct for intra-gel and inter-gel variability and to normalize the concentration of the specific detected proteins to the total amount of protein present, we performed a total protein stain (TPS) with Serva Purple (Serva, Proteomics Consult) according to the instructions of the manufacturer. After the staining, dry blots were also scanned with the Bio-Rad ChemiDoc MP Imaging System.

Semiquantitative analysis. The protein bands were evaluated semiquantitatively by densitometry (Image Lab software) and then separately for monocular and binocular cortex samples (Fig. 1*B*). First, to account for intra-gel and inter-gel variability including loading differences, incomplete transfer, or position on the blot, a TPS was used rather than the use of a single reference protein (Aldridge et al., 2008; Hu et al., 2011). For each protein of interest, the OD value per mouse was normalized to its corresponding TPS. Also, to compare samples between different gels, normalized data were expressed relative to the reference sample, i.e., a pool of all samples.

Pharmacological activation of the $GABA_A$ receptor α1 subunit in vivo

Indiplon is a synthetic "non-benzodiazepine," positive allosteric modulator that is highly selective for the α1 subunit-containing $GABA_A$ receptors (Foster et al., 2004; Sullivan et al., 2004; Petroski et al., 2006). We administered a daily dose of indiplon (9.5 mg/kg; Tocris Bioscience) intraperitoneally to a group of adult ME mice ($n = 5$). This manipulation

spanned the last 3 weeks of the 7 weeks post-enucleation survival period (see Fig. 6*A*). A control group ($n = 5$) was included that received vehicle solution (sunflower seed oil) injections. All injections were given in a volume of 10 ml/kg. Because indiplon penetrates through the blood–brain barrier and has sedative properties (Foster et al., 2004), we used locomotion activity as a readout for indiplon effectiveness. Circadian cage activity (see Fig. 6*B*) was measured by placing mice individually in 26.7 × 20.7 cm transparent cages (floor area, 370 cm^2) that were surrounded by three infrared photo beams. Beam crossings, which represented locomotion activity, were registered for each 15 min interval, during a 23 h recording period each day using an interfaced personal computer (Goddyn et al., 2006). After the 3 week injection period, brains were collected and prepared for ISH experiments.

Statistics

For each condition, the data of relative ODs were presented as mean ± SEM. A normal distribution was verified, and parallel equal variance between groups was tested. In the ISH analysis, when the test requirements were fulfilled, a two-way ANOVA was used with the factors subdivision (functional: binocular zone, medial or lateral monocular zone) and deprivation (AMC or 7wME) to test for ME-specific changes in *zif268* expression. Fisher's least significant difference (LSD) *post hoc* tests were used. When criteria for a parametric test were not fulfilled in both the Western blot and ISH analysis, a nonparametric Kruskal–Wallis test with Dunn's *post hoc* test or a Mann–Whitney *U* rank-sum test for pairwise comparison of independent samples was applied. When after a two-way ANOVA no interaction between the two factors studied was observed or if a parametric test was allowed, a one-way ANOVA with Fisher's LSD or Tukey's HSD *post hoc* tests or an unpaired Student's *t* test for pairwise comparison was used. For all tests, a probability level (α level was set to 0.05) of <0.05 was accepted as statistically significant ($^*p < 0.05$, $^{**}p < 0.01$, $^{***}p < 0.001$). Statistical analyses were performed using SigmaStat 3.1 (Systat Software).

Results

Recently, we reported a striking phenotypic variation in the response of adolescent (P45) and adult (P120) mice to ME (Nys et al., 2014). The readout consisted of a quantitative *zif268* expression-based comparison of subregion-specific activity levels in the contralateral visual cortex of ME mice with "age at onset" and "time after lesion" as variable factors. When initiated at P45, ME induces a persistent decrease in activity in the contralateral visual cortex (Fig. 1*F*,*G*), especially in its monocular regions (V2Lm, V1m, and V2M). In contrast, at 7 weeks after ME induction, P120 mice display a neuronal activity level (Fig. 1*F*,*G*) that closely resembles that of control (AMC) mice. Thus, an incomplete versus an extensive reactivation pattern typifies the contralateral visual cortex of adolescent and adult 7wME mice, respectively. This prompted us to examine whether local GABAergic inhibition acts as a brake on cross-modal plasticity in P45 mice and is relaxed in P120 mice, thereby permitting multimodal inputs to actively contribute to the post-ME reactivation process.

Dark exposure in adulthood reinstates a P45-like response to long-term ME

To non-invasively alter inhibitory neurotransmission, we applied a DE pretreatment. We questioned whether 10 d of complete visual deprivation by DE before ME would affect the response to ME in P120 mice. Our a priori assumption was that it would rejuvenate the response, as when applied before MD in adult rats to reopen the critical period for ocular dominance plasticity (He et al., 2006, 2007; Huang et al., 2010). In our ME model, if DE would rejuvenate the response to a P45-like state, less reactivation of especially the medial monocular visual cortex was to be expected.

To simplify interpretation of our dataset concerning the effect of DE in combination with ME, we first compared the experience-induced *zif268* expression levels in four types of controls, namely the P45 and P120 AMCs, as well as the DE C and DE AMC conditions (Fig. 1*H*,*I*). If comparable, this would allow comparison with one of the control conditions for interpretation of combined DE–ME effects. For the upper layers, the four activity profiles followed a similar trend along the lateromedial extent of the visual cortex (Fig. 1*H*; ANOVA on ranks: V2Lb, $p = 0.674$; V1b, $p = 0.359$; V1m, $p = 0.141$), except for the outermost subregions (Fig. 1*H*; ANOVA on ranks: V2Lm, $p = 0.024$; V2M, $p = 0.023$). For the lower layers, the four activity profiles also followed the same trend (Fig. 1*I*; ANOVA on ranks: V2Lm, $p = 0.481$; V2Lb, $p = 0.832$; V1b, $p = 0.562$; V1m, $p = 0.560$; V2M, $p = 0.110$). Therefore, DE per se does not seem to have an effect on visually evoked *zif268* expression in the visual cortex of normally sighted control mice, which allowed us to determine the effect of DE combined with ME in mice by comparing their reactivation profiles with DE AMC and P120 ME mice only (Fig. 1*F*,*G*).

ME after DE resulted in a vastly different outcome in P120 mice (Fig. 1*E*–*G*). The activity profile of the DE adult visual cortex revealed a lower *zif268* signal 7 weeks after ME compared with DE AMC (Fig. 1*E*). There was a significant interaction effect of ME on different cortical subdivisions in upper (Fig. 1*F*; two-way ANOVA: $F_{(1,4)} = 4.11$, $p = 0.007$) and lower (Fig. 1*G*; two-way ANOVA: $F_{(1,4)} = 3.44$, $p = 0.017$) layers. All layers of both the lateral (V2Lm) and medial monocular (V1m and part of V2M) cortices revealed decreased neuronal activity in DE 7wME compared with DE AMC (Fig. 1*F*; upper layers: V2Lm, $p < 0.001$; V1m, $p < 0.001$; V2M, $p < 0.001$; Fig. 1*G*; lower layers: V2Lm, $p < 0.001$; V1m, $p < 0.001$; V2M, $p < 0.001$). Likewise, comparison of the DE 7wME with P120 7wME mice revealed much lower *zif268* levels in the DE subjects (Fig. 1*F*; *t* test, upper layers: V2Lm, $p = 0.001$; V1m, $p < 0.001$; V2M, $p < 0.001$; Fig. 1*G*; lower layers: V2Lm, $p < 0.001$; V1m, $p < 0.001$; V2M, $p < 0.001$).

The binocular cortex of DE 7wME mice also displayed a significantly lower activity level than that of DE AMC (Fig. 1*F*; upper layers: V2Lb, $p = 0.002$; V1b, $p < 0.001$; Fig. 1*G*; lower layers: V2Lb, $p = 0.011$; V1b, $p = 0.014$) or P120 7wME group (infragranular layers only; Fig. 1*F*; *t* test, upper layers: V2Lb, $p = 0.122$; V1b, $p = 0.616$; Fig. 1*G*; *t* test, lower layers: V2Lb, $p = 0.006$; V1b, $p = 0.001$).

To facilitate direct comparison of the effect of age and DE, the left visual cortex activity levels of each enucleated group were normalized to their AMCs (7wME/AMC ratio; Fig. 2*A*–*F*). P45 and DE 7wME mice displayed a profound effect of unilateral enucleation across all cortical layers, especially for the lateral and medial monocular cortices (Fig. 2*A*,*C*,*D*,*F*). A much better recovery of *zif268* expression levels predominantly characterized the P120 7wME mice. Indeed, the reactivation capacity of the lateral monocular zone (Fig. 2*A*; one-way ANOVA, upper layers: $F_{(2,15)} = 26.129$, $p < 0.001$; P45 vs P120, $p < 0.001$; DE vs P120, $p < 0.001$; Fig. 2*D*; one-way ANOVA, lower layers: $F_{(2,15)} = 28.481$, $p < 0.001$; P45 vs P120, $p < 0.001$; DE vs P120, $p < 0.001$) and the medial monocular zone (Fig. 2*C*; one-way ANOVA, upper layers: $F_{(2,15)} = 44.119$, $p < 0.001$; P45 vs P120, $p < 0.001$; DE vs P120, $p < 0.001$; Fig. 2*F*; one-way ANOVA, lower layers: $F_{(2,15)} = 18.631$, $p < 0.001$; P45 vs P120, $p < 0.001$; DE vs P120, $p < 0.001$) of DE adults was significantly lower when compared with normally reared P120 7wME mice. With regard to the binocular cortex, *zif268* labeling was significantly diminished in DE 7wME compared with normally reared P120 7wME (Fig. 2*B*; one-way

ANOVA, upper layers: $F_{(2,15)} = 9.571$, $p = 0.002$; $p = 0.024$; Fig. 2*E*: one-way ANOVA, $F_{(2,15)} = 9.681$, $p = 0.002$; lower layers, $p = 0.007$). Thus, DE adult 7wME mice much more resembled P45 7wME mice because no significant difference in reactivation was found between adult dark-exposed enucleated and P45 enucleated mice, except for a more intense signal for dark-exposed adults in the upper layers of medial monocular cortex (Fig. 2*C*; DE vs P45, $p = 0.012$).

Summarized, DE before long-term ME in adulthood significantly reduced visual cortex reactivation. As such, the DE strategy converted the adult visual cortex in a more P45-like state in which the multimodal facet of ME-induced reactivation, typical for normally reared adults (Fig. 1*A–C*), is mainly lacking.

The effect of DE on nonvisual cortex activity after long-term ME

Previously, we demonstrated that the activity level of other sensory cortices is also age-specifically altered after long-term ME (Nys et al., 2014). Based on *zif268* expression, the highest activity levels in S1 and Au cortices were present in adult 7wME mice in which visual cortex reactivation includes cross-modal plasticity (Figs. 1*A*, 2*G*,*H*). Therefore, we assessed whether DE in adulthood also converted the response of the nonvisual sensory areas into lower P45-like activity levels in both S1 and Au (Fig. 2*G*,*H*; Nys et al. 2014). A significantly lower activity was detected in the auditory cortex of adult DE 7wME compared with DE AMC mice (Fig. 2*G*; rank-sum test, $p = 0.032$), whereas *zif268* expression appeared unchanged in the somatosensory cortex between these conditions (Fig. 2*H*; rank-sum test, $p = 1.000$). Auditory cortex activity in dark-exposed animals was, as in P45, significantly reduced compared with P120 7wME mice (Fig. 2*G*; one-way ANOVA, $F_{(2,13)} = 17.537$, $p < 0.001$; DE vs P120, $p < 0.001$). The somatosensory cortex also demonstrated a significant decline of *zif268* induction when adults were dark exposed before enucleation (Fig. 2*H*; one-way ANOVA, $F_{(2,13)} = 39.039$, $p < 0.001$; DE vs P120, $p = 0.002$). In summary, as predicted, DE 7wME mice did not develop the increased activity levels normally present in adult 7wME (Fig. 2*H*). Unlike most visual areas and auditory cortex, S1 activity in DE 7wME mice was still significantly higher than in P45 7wME mice (Fig. 2*H*; $p < 0.001$), indicating that the shift toward a P45-like response to ME could only be partial for this aspect.

Together, nonvisual cortices did not develop an increased activity level in adolescent and dark-exposed adult ME mice, supporting our interpretation that visual cortex reactivation in these two experimental groups mainly lacks the cross-modal component because of lower S1 and Au output toward visual areas to drive a full reactivation of monocular cortical territory.

Long-term ME induces distinct changes in inhibitory protein expression in the deprived medial monocular and binocular cortex

In the binocular cortex of adult rats, several studies reported that DE alters the quantity and quality of GABAergic transmission to enable ocular dominance plasticity in response to short-term MD by lid suture (He et al., 2006; Huang et al., 2010). However, how DE preceding long-term ME affects inhibitory factors in the medial monocular cortex, an area that receives input from only one eye and from nonvisual or multimodal areas (Wagor et al., 1980; Paperna and Malach, 1991; Van Brussel et al., 2011; Yoshitake et al., 2013), remains elusive. To begin to explore the mechanisms behind adult cross-modal plasticity in the late phase of recovery from ME, we compared the relative expression of inhibition-related proteins in DE 7wME mice with those in the enucleated P45 and P120 groups by means of immunoblotting.

Of particular relevance for the strength of inhibition at the presynaptic level is the GABA synthesizing enzyme GAD, which is present in two functionally distinct isoforms, GAD65 and GAD67, that have differential subcellular distribution patterns (Feldblum et al., 1993; Esclapez et al., 1994). Although GAD67 produces the majority of GABA throughout interneurons, GAD65 is specialized for the on-demand high production of GABA at axon terminals (Reetz et al., 1991; Wu et al., 2007; Kanaani et al., 2008). In binocular cortex homogenates, the expression of the two GAD protein isoforms remained unchanged (Fig. 3*F–I*). However, in the medial monocular cortex, GAD65 (Fig. 3*A*,*C*) was increased significantly after ME compared with AMCs in P45, DE, and normally reared P120 mice (Fig. 3*C*; *t* test, P45, $p = 0.032$; DE, $p = 0.0214$; P120, $p = 0.0361$). Cytosolic GAD67 (Fig. 3*A*,*D*) displayed a similar ME-induced increase relative to the AMC groups (Fig. 3*D*; rank-sum test, DE, $p = 0.0422$; P120, $p = 0.0302$), although this trend was not significant in adolescent mice (P45, $p = 0.0711$). These observations could reflect an ME-evoked increase in GABA production for fast release at axon terminals in the medial monocular cortex but not in the binocular visual cortex (Wu et al., 2007).

No significant differences in GAD65 and GAD67 expression were discerned between the three normalized ME groups (Fig. 3*C*; one-way ANOVA, $F_{(2,16)} = 0.600$, $p = 0.561$; Fig. 3*D*, one-way ANOVA, $F_{(2,16)} = 0.300$, $p = 0.745$; Fig. 3*H*; one-way ANOVA, $F_{(2,16)} = 1.566$, $p = 0.241$; Fig. 3*I*, one-way ANOVA, $F_{(2,16)} = 0.307$, $p = 0.740$). Also, no "DE only" effect was observed (Fig. 5*A*,*B*), substantiating that this regulation of GAD expression within the medial monocular cortex is age and dark experience independent, but ME dependent, in our long-term ME model.

Given that the VGAT is responsible for loading GABA into synaptic vesicles, it comprises another level of regulation of GABA release. P45 and DE mice displayed a similar increasing trend in VGAT expression after long-term ME in binocular cortex homogenates, not observed in P120 ME mice (Fig. 3*J*; one-way ANOVA, $F_{(2,16)} = 0.\ 5.793$, $p = 0.013$). Thus, the binocular cortex exhibits a DE-induced rejuvenation of adult VGAT protein expression toward P45 levels. Conversely, the medial monocular cortex adapted differently from ME, regardless of age, because the amount of VGAT (Fig. 3*B*,*E*) was significantly downregulated in P120 (rank-sum test, $p < 0.001$), P45 (rank-sum test, $p = 0.0221$), and DE (rank-sum test, $p = 0.0260$) ME mice relative to AMCs. The effect of DE in combination with ME appears to be additive because DE per se already induced persistent alterations in VGAT levels in the medial monocular cortex (Fig. 5*C*), and the differences in the ratios are attributable to significantly decreased levels of the transporter in DE AMC compared with P45 AMC and P120 AMC (one-way ANOVA for AMC groups, $F_{(3,20)} = 6.943$, $p = 0.0022$) mice. Accordingly, comparison of the three ME-groups (ME/AMC ratios) showed a significant difference of VGAT levels between dark-exposed and normally reared adult enucleated mice (Fig. 3*E*; one-way ANOVA, $F_{(2,16)} = 0.300$, $p = 0.745$).

In relation to GABA signaling at the postsynaptic site, the $\alpha 1$ subunit of the ionotropic $GABA_A$ receptor predominantly mediates fast hyperpolarization typical for phasic inhibition on both pyramidal and inhibitory neurons. The $GABA_A$ receptor $\alpha 1$ subunit is most abundant in the mature visual cortex (Laurie et al.,

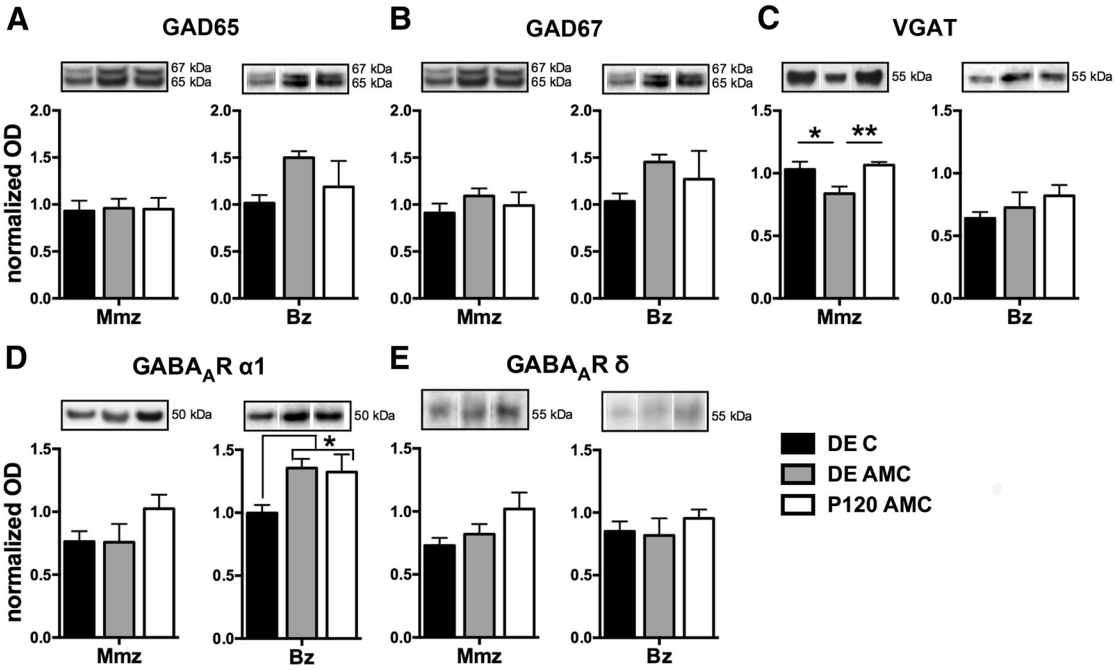

Figure 5. The effect of DE on different inhibitory proteins in the Mmz and Bz. ODs of WB results for GAD65 (***A***), GAD67 (***B***), VGAT (***C***), the $GABA_A$ receptor α1 subunit (***D***), and the δ subunit (***E***) in DE C (black), DE AMC (gray), and P120 AMC (white) mice are shown. Representative Western blot bands from functional subdivision-specific homogenates and their molecular weight are depicted above the bar graphs. In the medial monocular cortex, a significantly reduced expression of VGAT in the DE AMC mice compared with the other two controls was discerned. In the binocular cortex, a significant decrease of the $GABA_A$ receptor α1 subunit was present directly after DE (DE C).

1992; Wisden et al., 1992; Dunning et al., 1999; Chen et al., 2001; Conti et al., 2004; Heinen et al., 2004; Bosman et al., 2005) and is implicated strongly in the timing of inhibition-controlled ocular dominance plasticity in the mouse binocular cortex (Hensch et al., 1998; Fagiolini and Hensch, 2000; Iwai et al., 2003; Fagiolini et al., 2004; Katagiri et al., 2007). In the medial monocular cortex of 7wME mice, age and DE similarly affected the $GABA_A$ receptor α1 subunit expression because a significant upregulation was found in P45 and DE mice when compared with their AMCs (Fig. 4*A*,*C*; *t* test, P45, $p = 0.0038$; DE, $p = 0.00117$). The α1 expression was not altered in P120 7wME mice (*t* test, $p = 0.419$). Therefore, the elevated expression of the α1 subunit correlates with the incomplete cortical reactivation and thus a lack of cross-modal recovery in the medial monocular cortex. Different observations were made for the binocular cortex. A comparison of the normalized ratios for protein levels of the $GABA_A$ receptor α1 subunit (Fig. 4*E*,*G*) after long-term ME indicated a significantly higher ratio in P45 compared with the adult DE and P120 groups (Fig. 4*G*; one-way ANOVA, $F_{(2,16)} = 0.\ 8.966$, $p = 0.002$). Thus, no similarity between the ratio of P45 and DE mice was detected, again suggesting cortical region-specific adaptations of inhibitory proteins to ME.

We next examined the expression of the functionally distinct $GABA_A$ receptor subunit δ (Fig. 4*B*,*D*,*F*,*H*). This subunit has an additional role in the nature of inhibition because it selectively mediates tonic inhibition of both pyramidal and inhibitory neurons in the neocortex (Wei et al., 2003; Semyanov et al., 2004; Brickley and Mody, 2012). There was no difference in $GABA_A$ receptor subunit δ expression in either medial monocular (Fig. 4*D*; ME vs AMC, *t* test, P45, $p = 0.4248$; rank-sum test, DE, $p = 0.6667$; *t* test, P120, $p = 0.303$; Fig. 4*D*; one-way ANOVA, $F_{(2,16)} = 1.188$, $p = 0.3336$; Fig. 5*E*) or binocular visual (Fig. 4*H*; ME vs AMC, *t* test, P45, $p = 0.2734$; *t* test, DE, $p = 0.1465$; *t* test, P120, $p = 0.8256$; Fig. 4*H*; one-way ANOVA, $F_{(2,16)} = 1.217$, $p = 0.322$; Fig. 5*E*) cortex for any of the experimental conditions .

In summary, binocular and monocular cortices do not respond uniformly in terms of long-term expression changes for inhibitory marker proteins as manifested during ME. This could suggest intrinsic differences in GABAergic plasticity and stability across these two functionally distinct cortical regions that in turn could relate to their distinct capacity for experience-dependent plasticity.

DE effect on the expression of GABAergic markers in monocular versus binocular visual cortex of control mice

Our indications for an enhanced inhibitory tone by DE combined with ME on the medial monocular cortex of adult mice appeared at odds with previous reports for binocular visual cortex of adult rats, in which DE diminishes GABAergic proteins and synaptic transmission (He et al., 2006; Huang et al., 2010). Therefore, we also evaluated the effect of DE on the expression of the different inhibitory protein markers in three relevant control groups (DE C, DE AMC, and P120 AMC) and then in parallel for monocular and binocular cortices (Fig. 5*A*–*E*). Consistent with the study by He et al. (2006) that showed decreased levels of the $GABA_A$ receptor β2/3 subunit relative to GluR2 in adult rats (He et al., 2006), we also found a significant reduction in $GABA_A$ receptor α1 subunit levels and this specifically in the binocular cortex immediately after the DE period (DE C) compared with P120 and DE AMCs (Fig. 5*D*, Bz; one-way ANOVA, $F_{(2,17)} = 3.997$, $p = 0.041$). This confirms that darkness in adulthood lowers inhibitory proteins in binocular cortex, yet this finding does not hold for the monocular visual cortex (Fig. 5*D*, Mmz; one-way ANOVA, $F_{(2,17)} = 1.691$, $p = 0.218$). Although we also expected reduced VGAT levels after DE in the binocular cortex based on the study by Huang et al. (2010), this was not evident in our

dataset (Fig. 5*C*). Nevertheless, a rather long-term reduction effect of DE followed by normal visual experience (DE AMC) on VGAT protein expression was detected in the monocular cortex (Fig. 5*C*, Mmz; one-way ANOVA, $F_{(2,14)} = 5.729$, $p = 0.018$). No changes for any of the other presynaptic and postsynaptic inhibitory marker proteins were detected. Of note, given the findings for DE, the earlier observation for a decreasing trend in the ratio of the $GABA_A$ receptor $\alpha1$ subunit level in the binocular cortex of DE 7wME animals (Fig. 4*G*) may be the result of DE (Fig. 5*D*) rather than the combined effect of DE with ME. Thus, these findings support the interpretation that monocular and binocular visual cortices adapt differently to visual deprivation by DE.

Pharmacological stimulation of $\alpha1$ subunit-containing $GABA_A$ receptors in adult ME mice impairs extensive long-term reactivation

Based on the biochemical results (Fig. 4*A*,*C*), we hypothesized that increasing $\alpha1$-containing $GABA_A$ receptor transmission could provide a way to at least partially mimic the effect of DE on ME-induced reactivation of the monocular visual cortex. Therefore, we performed a pharmacological experiment as an additional approach to manipulate and confirm a role for GABAergic transmission in ME-induced plasticity (Fig. 6). The $GABA_A$ $\alpha1$ subunit-selective agonist indiplon was administered systemically in adult enucleated mice and then once a day during the last 3 weeks of the 7 week ME period, the timeframe of the cross-modal events in adult ME mice (Figs. 1*A–C*, 6*A*). To assess indiplon efficiency, circadian locomotion activity was first measured. The compound persistently affected this activity, especially during the first hours of the dark phase of the circadian cycle (Fig. 6*B*). This was reflected by a significant decline in total beam crossings of the indiplon-injected mice compared with the sham group at day 1 (Fig. 6*B*,*C*; *t* test, $p = 0.0018$) up to day 20 (Fig. 6*C*; *t* test, $p = 0.0046$). Endpoint activity mapping revealed a significant indiplon-dependent decrease in medial (Fig. 6*J*, Mmz; *t* test, $p = 0.0139$) and lateral (Fig. 6*H*, Lmz; *t* test, $p < 0.001$) monocular cortex activity across the infragranular layers only compared with the activation level of adult 7wME. In addition, the somatosensory cortex demonstrated a significant decline of *zif268* induction across all cortical layers (Fig. 6*G*; *t* test, upper layers, $p < 0.001$; Fig. 6*K*; *t* test, lower layers, $p < 0.001$). Hence, reduced S1 output could limit the nonvisual drive for cross-modal reactivation in the medial monocular cortex. Nonetheless, the layer- and cortical region-specific effect in the visual cortex combined with the decreased activity in S1 of indiplon-treated adult ME mice do suggest suppression of the late cross-modal potentiation phase in the monocular cortex of P45 and DE adult mice by intracortical inhibition.

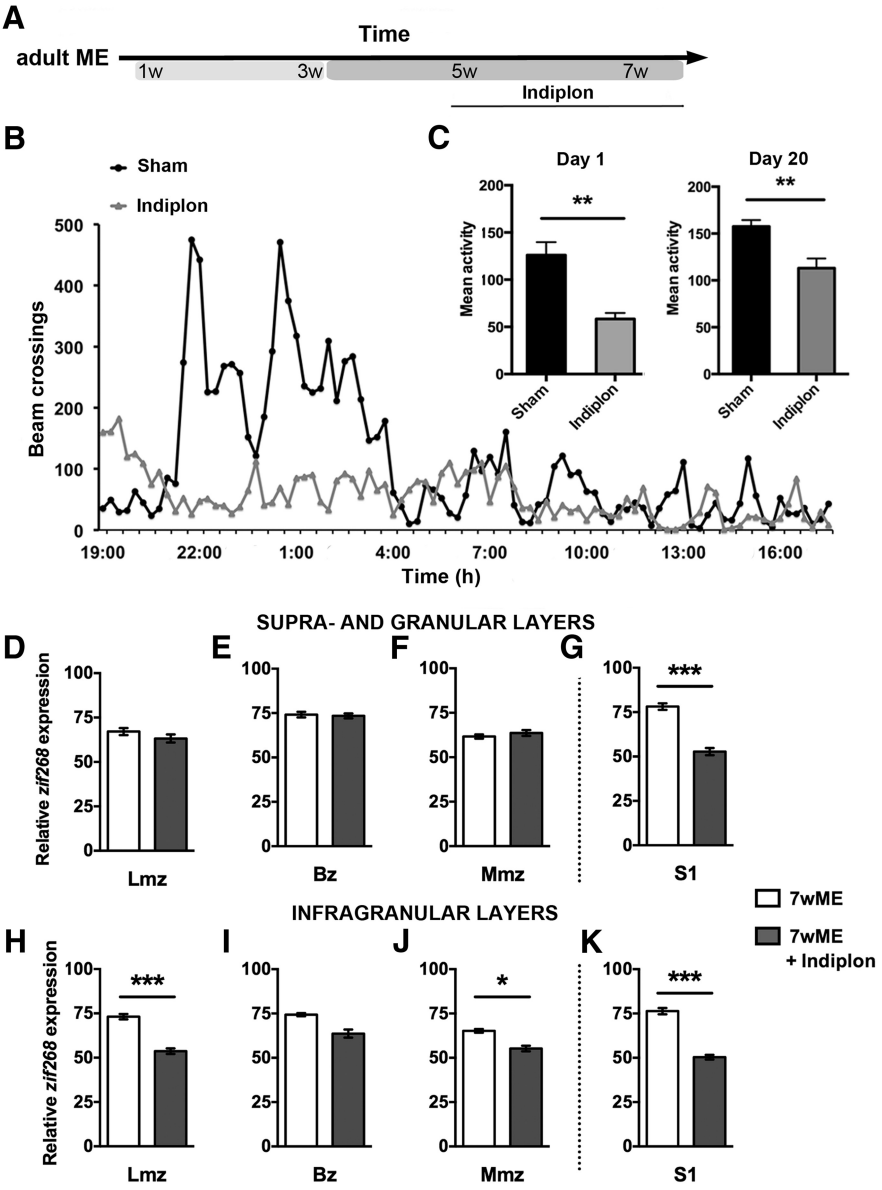

Figure 6. Pharmacological stimulation of $\alpha1$ subunit-containing $GABA_A$ receptors in adult ME mice partially reduces the adult-specific extensive reactivation and decreases somatosensory cortex activation. ***A***, Design of the pharmacological experiment in adult (P120) mice in relation to the weeks after ME. ***B***, Circadian locomotion activity of sham (black) and indiplon-injected (gray) mice is depicted for day 1. ***C***, Comparison of the total counts of beam crossings (mean activity) at day 1 up to the end of the period (day 20) revealed hypoactivity at the locomotion level in the indiplon group (gray), confirming its effectiveness *in vivo*. Cortical activity patterns as measured by means of ISH for the activity reporter *zif268* (***D–K***) unraveled a significant decrease in visual cortex reactivation across the infragranular layers of the medial (***J***) and lateral monocular (***H***) cortices, as well as a significant drop in activity across both the upper (***G***) and lower (***K***) layers of somatosensory area S1.

Discussion

The molecular mechanisms regulating deprivation-induced cross-modal plasticity in the sensory neocortex have not yet been resolved. We witnessed an overt brain region-specific effect of ME on the expression of proteins related to GABAergic transmission in the monocular and binocular cortices. Our molecular approaches revealed specifically how increased $GABA_A$ receptor $\alpha1$ subunit expression and exogenous activation prevents a cross-modal takeover of the monocular cortex in adolescent and indiplon-treated adult ME mice, respectively. The inhibitory limitation in P45 appears re-

laxed in adulthood, thereby permitting nonvisual inputs to slowly reactivate the medial monocular cortex, once unimodal plasticity based on open eye potentiation has ceased.

Inhibitory marker proteins are affected differently in the medial monocular and binocular cortices

Recalibration of the excitation–inhibition balance is established by activity-dependent modifications in local and long-range intracortical connectivity patterns of GABAergic and pyramidal neurons and is of particular importance to neuronal plasticity (Trachtenberg et al., 2000; Calford et al., 2003; Keck et al., 2011; Vasconcelos et al., 2011). Overall, in the binocular cortex, a 7 week recovery period after ME appeared sufficient to reestablish an inhibitory status similar to AMC levels. The binocular cortex of P45, P120, or DE 7wME mice displayed only minor long-term expression changes for any of the inhibition markers investigated. The age and/or DE effects that occurred, such as for VGAT or the $GABA_A$ receptor α1 subunit, were clearly different from those in the medial monocular cortex. Indeed, long-term ME specifically increased GAD protein expression regardless of age or DE in the medial monocular cortex. Increased GAD levels likely correspond to GABA production above normal levels and are suggestive of an upregulation of the on-demand high production of vesicular GABA, particularly provided by GAD65 at axon terminals (Soghomonian and Martin, 1998; Wu et al., 2007; Kanaani et al., 2008). In the monocular cortex of both normally reared and dark-exposed adult ME mice, the rise in GAD67 could indicate more GABA synthesis throughout interneurons for the purpose of both nonvesicular and vesicular release and for metabolic demands (Belhage et al., 1993; Lau and Murthy, 2012). VGAT expression showed an ME-evoked decrease only in the monocular cortex. This transporter is functionally coupled to GAD65 (Chaudhry et al., 1998; Jin et al., 2003; Hartmann et al., 2008) to load GABA into synaptic vesicles and is defined as a marker for presynaptic inhibitory contacts (Micheva et al., 2010). Possibly, the decline in VGAT in the monocular cortex corresponds to a subtype(s)-specific or a uniform reduction in density of presynaptic GABAergic terminals. From a functional perspective, future investigations of a potential redistribution of GABA signaling among different interneuron subtypes, in which some interneurons produce and release more GABA whereas others retract their terminals, are of interest. An alternative explanation could be that ME decreased VGAT at individual existing synapses without significantly altering the density of inhibitory contacts (Tabuchi et al., 2007; Blundell et al., 2009). In this situation, and in combination with the upregulation of GAD65, it could suggest an activity-dependent regulation of quantal size resulting from a higher GABA accumulation in less vesicles in the medial monocular cortex (Cherubini and Conti, 2001). Long-term alterations in favor of inhibition have already been attributed to particular late aspects of cortical reorganization in other studies (Benali et al., 2008). For instance, in the V1 of adult retinal lesion cats, GABA levels measured by *in vivo* microdialysis initially decrease before increasing to values that exceed normal levels to possibly counteract synchronous hyperexcitability (Arckens et al., 2000a; Massie et al., 2003b).

The distinct response of the monocular and binocular cortices to long-term ME in terms of GABAergic protein expression further suggests a different degree of local inhibitory modulation or stabilization. Accordingly, the synaptic threshold for the induction of LTP in the rat visual cortex is lower in the binocular cortex than in the monocular cortex (Kuo and Dringenberg, 2012). Our findings support an age- and cortical region-specific regulatory role for inhibition in ME-induced cortical reorganization and further corroborate the growing evidence for distinct plasticity phenomena in the functional subregions of the mouse visual cortex, as reported previously for tree shrew (McCoy et al. 2008) and mouse (Nataraj and Turrigiano, 2011; Yoshitake et al., 2013; Nys et al., 2014). A different recruitment of inhibitory neurons inside the monocular and binocular cortices has also been reported in the context of learning-induced visual cortex plasticity in the mouse (Liguz-Lecznar et al., 2009).

Our observations for the inhibitory markers mainly suggest that the DE effect combined with ME is in favor of inhibition in the monocular cortex opposite to its effect on short-term MD-induced plasticity in binocular cortex, which is in favor of excitation (He et al., 2006). Reduced sensory input leads to an altered regimen of neural activity that has a pronounced effect on monocular cortex activation and would depend on the mechanisms different from those underlying ocular dominance plasticity. Potential candidates are homeostatic synaptic scaling on a rapid timescale (Turrigiano et al., 1998; Goel et al., 2006; Maffei and Fontanini, 2009; Mrsic-Flogel et al., 2007; Keck et al., 2013) and multimodal plasticity on a longer timescale (Van Brussel et al., 2011).

DE hampers the reactivation of the adult medial monocular cortex in response to long-term ME

The long-range multimodal projections to the visual cortex (Wagor et al., 1980; Paperna and Malach, 1991; Larsen, 2009; Campi et al., 2010; Laramée et al., 2011, 2013; Van Brussel et al., 2011; Charbonneau et al., 2012; Iurilli et al., 2012; Henschke et al., 2014; Stehberg et al., 2014) represent an adequate substrate for recruiting alternative cortical inputs that take part in the reactivation of the adult deprived visual cortex. Indeed, whisker manipulations after long-term ME revealed a strong involvement of somatosensory input in the late, cross-modal aspect of the reactivation response to ME (Fig. 1*A–C*; Van Brussel et al., 2011). However, this mechanism is not recruited, nonfunctional, less engaged, or different in nature in P45 and DE adult ME mice. The parallel observation that nonvisual cortices (S1, Au) also display lower activity levels exactly in the adolescent and dark-exposed adult ME conditions further supports our interpretation of a visual cortex reactivation that is confined predominantly to the open eye potentiation principle and therefore remains partial.

An inhibitory brake on cross-modal plasticity in P45 and DE mice?

We have linked the incomplete reactivation of the visual cortex typical for P45 ME and DE adult ME animals to an increased expression of the α1 subunit of the $GABA_A$ receptor relative to AMCs. Moreover, pharmacological enhancement of the $GABA_A$ receptor α1-mediated transmission with indiplon during the late cross-modal phase of recovery after ME in adult mice was sufficient to specifically diminish the typical reactivation profile especially in the infragranular layers of the medial and lateral monocular visual cortices. The lower layers have been well correlated with cross-modal driven plasticity because they are most affected by ME and whisker manipulations subsequent to ME in adult mice (Fig. 1*A–C*; Van Brussel et al., 2011). The indiplon treatment also prevented increased activity in S1, which indirectly could have contributed to less tactile output, normally responsible for driving the cross-modal reactivation of the medial visual cortex. Nevertheless, our observations still emphasize a central role for $GABA_A$ receptor α1 subunit-mediated inhibition

in the ability for cross-modal plasticity in adult mice. Fast-spiking interneurons could be involved because their axon terminals are opposed to the α1 subunit-containing $GABA_A$ receptors. This receptor subtype predominantly mediates fast hyperpolarization and phasic inhibition at the proximal dendrites or somata of pyramidal and GABAergic neurons (Nusser et al., 1996; Okada et al., 2000; Cherubini and Conti, 2001; Klausberger et al., 2002). The fast-spiking interneurons often represent basket cells that in turn mostly comprise parvalbumin-positive interneurons (Markram et al., 2004; Druga, 2009).

The underlying network properties of interneurons at the time of enucleation may also contribute to the age-dependent phenotypic variation of the cortical reactivation. In fact, certain aspects of GABAergic maturation also encompass adolescence (Di Cristo, 2007; Okaty et al., 2009; Kilb, 2012). In rat and mouse, the inhibitory circuits of the visual cortex are functionally and structurally mature, but they are not recruited maximally by visual experience at P45, an age that has been linked to a refractory period for inhibitory plasticity (Huang et al., 2010; Gu et al., 2013). In humans, different developmental trajectories are present for GABAergic signaling mechanisms in V1 that continue well into adolescence (Murphy et al., 2005; Pinto et al., 2010). Interestingly, if prolonged MD is applied in kittens, it accelerates the maturation of the $GABA_A$ α1 receptor in the visual cortex representing the monocular visual field (Beston et al., 2010). Together, this could suggest that, at P45, ME provokes a long-term increase in inhibitory tone in the medial monocular cortex to accelerate or re-express certain functional aspects of inhibitory maturation. As a result, it is conceivable that a higher threshold (suboptimal) for excitatory afferents from other sensory cortices is generated locally or by long-range feedforward inhibition to keep the visual territory allegiant to its dominant sensory input.

References

Aerts J, Nys J, Arckens L (2014) A highly reproducible and straightforward method to perform *in vivo* ocular enucleation in the mouse after eye opening. J. Vis Exp 92:e51936. CrossRef Medline

Aldridge GM, Podrebarac DM, Greenough WT, Weiler IJ (2008) The use of total protein stains as loading controls: an alternative to high-abundance single-protein controls in semi-quantitative immunoblotting. J Neurosci Methods 172:250–254. CrossRef Medline

Arckens L, Zhang F, Vanduffel W, Mailleux P, Vanderhaeghen JJ, Orban GA, Vandesande F (1995) Localization of the two protein kinase C beta-mRNA subtypes in cat visual system. J Chem Neuroanat 8:117–124. CrossRef Medline

Arckens L, Schweigart G, Qu Y, Wouters G, Pow DV, Vandesande F, Eysel UT, Orban GA (2000a) Cooperative changes in GABA, glutamate and activity levels: the missing link in cortical plasticity. Eur J Neurosci 12: 4222–4232. CrossRef Medline

Arckens L, Van Der Gucht E, Eysel UT, Orban GA, Vandesande F (2000b) Investigation of cortical reorganization in area 17 and nine extrastriate visual areas through the detection of changes in immediate early gene expression as induced by retinal lesions. J Comp Neurol 425:531–544. CrossRef Medline

Belhage B, Hansen GH, Schousboe A (1993) Depolarization by K+ and glutamate activates different neurotransmitter release mechanisms in GABAergic neurons: Vesicular versus non-vesicular release of GABA. Neuroscience 54:1019–1034. CrossRef Medline

Benali A, Weiler E, Benali Y, Dinse HR, Eysel UT (2008) Excitation and inhibition jointly regulate cortical reorganization in adult rats. J Neurosci 28:12284–12293. CrossRef Medline

Beston BR, Jones DG, Murphy KM (2010) Experience-dependent changes in excitatory and inhibitory receptor subunit expression in visual cortex. Front Synaptic Neurosci 2:138. CrossRef Medline

Blundell J, Tabuchi K, Bolliger MF, Blaiss CA, Brose N, Liu X, Südhof TC, Powell CM (2009) Increased anxiety-like behavior in mice lacking the inhibitory synapse cell adhesion molecule neuroligin 2. Genes Brain Behav 8:114–126. CrossRef Medline

Bosman LW, Heinen K, Spijker S, Brussaard AB (2005) Mice lacking the major adult GABAA receptor subtype have normal number of synapses, but retain juvenile IPSC kinetics until adulthood. J Neurophysiol 94:338–346. CrossRef Medline

Brickley SG, Mody I (2012) Extrasynaptic GABAA receptors: their function in the CNS and implications for disease. Neuron 73:23–34. CrossRef Medline

Calford MB, Wright LL, Metha AB, Taglianetti V (2003) Topographic plasticity in primary visual cortex is mediated by local corticocortical connections. J Neurosci 23:6434–6442. Medline

Callaway EM (2004) Feedforward, feedback and inhibitory connections in primate visual cortex. Neural Networks 17:625–632. CrossRef Medline

Campi KL, Bales KL, Grunewald R, Krubitzer L (2010) Connections of auditory and visual cortex in the prairie vole (*Microtus ochrogaster*): evidence for multisensory processing in primary sensory areas. Cereb Cortex 20:89–108. CrossRef Medline

Charbonneau V, Laramée ME, Boucher V, Bronchti G, Boire D (2012) Cortical and subcortical projections to primary visual cortex in anophthalmic, enucleated and sighted mice. Eur J Neurosci 36:2949–2963. CrossRef Medline

Chaudhry FA, Reimer RJ, Bellocchio EE, Danbolt NC, Osen KK, Edwards RH, Storm-Mathisen J (1998) The vesicular GABA transporter, VGAT, localizes to synaptic vesicles in sets of glycinergic as well as GABAergic neurons. J Neurosci 18:9733–9750. Medline

Chaudhuri A, Matsubara JA, Cynader MS (1995) Neuronal activity in primate visual cortex assessed by immunostaining for the transcription factor Zif268. Vis Neurosci 12:35–50. CrossRef Medline

Chen L, Yang C, Mower GD (2001) Developmental changes in the expression of GABAA receptor subunits (alpha1, alpha2, alpha3) in the cat visual cortex and the effects of dark rearing. Mol Brain Res 88:135–143. CrossRef Medline

Cherubini E, Conti F (2001) Generating diversity at GABAergic synapses. Trends Neurosci 24:155–162. CrossRef Medline

Cole AJ, Saffen DW, Baraban JM, Worley PF (1989) Rapid increase of an immediate early gene messenger RNA in hippocampal neurons by synaptic NMDA receptor activation. Nature 340:474–476. CrossRef Medline

Conti F, Minelli A, Melone M (2004) GABA transporters in the mammalian cerebral cortex: localization, development and pathological implications. Brain Res Rev 45:196–212. CrossRef Medline

Datwani A, McConnell MJ, Kanold PO, Micheva KD, Busse B, Shamloo M, Smith SJ, Shatz CJ (2009) Classical MHCI molecules regulate retinogeniculate refinement and limit ocular dominance plasticity. Neuron 64: 463–470. CrossRef Medline

Desgent S, Boire D, Ptito M (2010) Altered expression of parvalbumin and calbindin in interneurons within the primary visual cortex of neonatal enucleated hamsters. Neuroscience 171:1326–1340. CrossRef Medline

Di Cristo G (2007) Development of cortical GABAergic circuits and its implications for neurodevelopmental disorders. Clin Genet 72:1–8. CrossRef Medline

Druga R (2009) Neocortical inhibitory system. Folia Biol (Praha) 55:201–217. Medline

Dunning DD, Hoover CL, Soltesz I, Smith MA, O'Dowd DK (1999) GABAA receptor-mediated miniature postsynaptic currents and alpha-subunit expression in developing cortical neurons. J Neurophysiol 82:3286–3297. Medline

Esclapez M, Tillakaratne NJ, Kaufman DL, Tobin AJ, Houser CR (1994) Comparative localization of two forms of glutamic acid decarboxylase and their mRNAs in rat brain supports the concept of functional differences between the forms. J Neurosci 14:1834–1855. Medline

Fagiolini M, Hensch TK (2000) Inhibitory threshold for critical-period activation in primary visual cortex. Nature 404:183–186. CrossRef Medline

Fagiolini M, Fritschy JM, Löw K, Möhler H, Rudolph U, Hensch TK (2004) Specific GABAA circuits for visual cortical plasticity. Science 303:1681–1683. CrossRef Medline

Feldblum S, Erlander MG, Tobin AJ (1993) Different distributions of GAD65 and GAD67 mRNAs suggest that the two glutamate decarboxylases play distinctive functional roles. J Neurosci Res 34:689–706. CrossRef Medline

Foster AC, Pelleymounter MA, Cullen MJ, Lewis D, Joppa M, Chen TK, Bozigian HP, Gross RS, Gogas KR (2004) In vivo pharmacological characterization of indiplon, a novel pyrazolopyrimidine sedative-hypnotic. J Pharmacol Exp Ther 311:547–559. CrossRef Medline

Franklin KB, Paxinos G (2008) The mouse brain in stereotactic coordinates, Ed 3. San Diego: Elsevier Academic.

Friedel P, Hemmen JL (2008) Inhibition, not excitation, is the key to multimodal sensory integration. Brain Struct Funct 98:597–618. CrossRef Medline

Goddyn H, Leo S, Meert T, D'Hooge R (2006) Differences in behavioural test battery performance between mice with hippocampal and cerebellar lesions. Behav Brain Res 173:138–147. CrossRef Medline

Goel A, Lee HK (2007) Persistence of experience-induced homeostatic synaptic plasticity through adulthood in superficial layers of mouse visual cortex. J Neurosci 27:6692–6700. CrossRef Medline

Goel A, Jiang B, Xu LW, Song L, Kirkwood A, Lee HK (2006) Cross-modal regulation of synaptic AMPA receptors in primary sensory cortices by visual experience. Nat Neurosci 9:1001–1003. CrossRef Medline

Gogolla N, Takesian AE, Feng G, Fagiolini M, Hensch TK (2014) Sensory integration in mouse insular cortex reflects GABA circuit maturation. Neuron 83:894–905. CrossRef Medline

Gu Y, Huang S, Chang MC, Worley P, Kirkwood A, Quinlan EM (2013) Obligatory role for the immediate early gene NARP in critical period plasticity. Neuron 79:335–346. CrossRef Medline

Hada Y, Yamada Y, Imamura K, Mataga N, Watanabe Y, Yamamoto M (1999) Effects of monocular enucleation on parvalbumin in rat visual system during postnatal development. Invest Ophthalmol Vis Sci 40: 2535–2545. Medline

Hartmann K, Bruehl C, Golovko T, Draguhn A (2008) Fast homeostatic plasticity of inhibition via activity-dependent vesicular filling. PLoS One 3:e2979. CrossRef Medline

He HY, Hodos W, Quinlan EM (2006) Visual deprivation reactivates rapid ocular dominance plasticity in adult visual cortex. J Neurosci 26:2951–2955. CrossRef Medline

He HY, Ray B, Dennis K, Quinlan EM (2007) Experience-dependent recovery of vision following chronic deprivation amblyopia. Nat Neurosci 10: 1134–1136. CrossRef Medline

Heinen K, Bosman LWJ, Spijker S, van Pelt J, Smit AB, Voorn P, Baker RE, Brussaard AB (2004) GABAA receptor maturation in relation to eye opening in the rat visual cortex. Neuroscience 124:161–171. CrossRef Medline

Hensch TK, Fagiolini M, Mataga N, Stryker MP, Baekkeskov S, Kash SF (1998) Local GABA circuit control of experience-dependent plasticity in developing visual cortex. Science 282:1504–1508. CrossRef Medline

Henschke JU, Noesselt T, Scheich H, Budinger E (2014) Possible anatomical pathways for short-latency multisensory integration processes in primary sensory cortices. Brain Struct Funct 220:955–977. CrossRef Medline

Huang S, Gu Y, Quinlan EM, Kirkwood A (2010) A refractory period for rejuvenating GABAergic synaptic transmission and ocular dominance plasticity with dark exposure. J Neurosci 30:16636–16642. CrossRef Medline

Hu TT, Van den Bergh G, Thorrez L, Heylen K, Eysel UT, Arckens L (2011) Recovery from retinal lesions: molecular plasticity mechanisms in visual cortex far beyond the deprived zone. Cereb Cortex 21:2883–2892. CrossRef Medline

Imbrosci B, Ytebrouck E, Arckens L, Mittmann T (2014) Neuronal mechanisms underlying transhemispheric diaschisis following focal cortical injuries. Brain Struct Funct. Advance online publication. Retrieved June 8, 2015. doi:10.1007/s00429-014-0750-8. CrossRef Medline

Iurilli G, Ghezzi D, Olcese U, Lassi G, Nazzaro C, Tonini R, Tucci V, Benfenati F, Medini P (2012) Sound-driven synaptic inhibition in primary visual cortex. Neuron 73:814–828. CrossRef Medline

Iwai Y, Fagiolini M, Obata K, Hensch TK (2003) Rapid critical period induction by tonic inhibition in visual cortex. J Neurosci 23:6695–6702. Medline

Jin H, Wu H, Osterhaus G, Wei J, Davis K, Sha D, Floor E, Hsu CC, Kopke RD, Wu JY (2003) Demonstration of functional coupling between gamma-aminobutyric acid (GABA) synthesis and vesicular GABA transport into synaptic vesicles. Proc Natl Acad Sci U S A 100:4293–4298. CrossRef Medline

Jitsuki S, Takemoto K, Kawasaki T, Tada H, Takahashi A, Becamel C, Sano A, Yuzaki M, Zukin RS, Ziff EB, Kessels HW, Takahashi T (2011) Serotonin mediates cross-modal reorganization of cortical circuits. Neuron 69:780–792. CrossRef Medline

Kaczmarek L, Chaudhuri A (1997) Sensory regulation of immediate-early gene expression in mammalian visual cortex: implications for functional mapping and neural plasticity. Brain Res Brain Res Rev 23:237–256. CrossRef Medline

Kanaani J, Patterson G, Schaufele F, Lippincott-Schwartz J, Baekkeskov S (2008) A palmitoylation cycle dynamically regulates partitioning of the GABA-synthesizing enzyme GAD65 between ER-Golgi and post-Golgi membranes. J Cell Sci 121:437–449. CrossRef Medline

Kanold PO, Kim YA, GrandPre T, Shatz CJ (2009) Co-regulation of ocular dominance plasticity and NMDA receptor subunit expression in glutamic acid decarboxylase-65 knock-out mice. J Physiol 587:2857–2867. CrossRef Medline

Katagiri H, Fagiolini M, Hensch TK (2007) Optimization of somatic inhibition at critical period onset in mouse visual cortex. Neuron 53:805–812. CrossRef Medline

Keck T, Scheuss V, Jacobsen RI, Wierenga CJ, Eysel UT, Bonhoeffer T, Hübener M (2011) Loss of sensory input causes rapid structural changes of inhibitory neurons in adult mouse visual cortex. Neuron 71:869–882. CrossRef Medline

Keck T, Keller GB, Jacobsen RI, Eysel UT, Bonhoeffer T, Hübener M (2013) Synaptic scaling and homeostatic plasticity in the mouse visual cortex in vivo. Neuron 80:327–334. CrossRef Medline

Kilb W (2012) Development of the GABAergic system from birth to adolescence. Neuroscientist 18:613–630. CrossRef Medline

Klausberger T, Roberts JDB, Somogyi P (2002) Cell type-and input-specific differences in the number and subtypes of synaptic $GABA_A$ receptors in the hippocampus. J Neurosci 22:2513–2521. Medline

Kuo MC, Dringenberg HC (2012) Comparison of long-term potentiation (LTP) in the medial (monocular) and lateral (binocular) rat primary visual cortex. Brain Res 1488:51–59. CrossRef Medline

Laramée ME, Kurotani T, Rockland KS, Bronchti G, Boire D (2011) Indirect pathway between the primary auditory and visual cortices through layer V pyramidal neurons in V2L in mouse and the effects of bilateral enucleation. Eur J Neurosci 34:65–78. CrossRef Medline

Laramée ME, Rockland KS, Prince S, Bronchti G, Boire D (2013) Principal component and cluster analysis of layer V pyramidal cells in visual and non-visual cortical areas projecting to the primary visual cortex of the mouse. Cereb Cortex 23:714–728. CrossRef Medline

Larsen DD, Luu JD, Burns ME, Krubitzer L (2009) What are the effects of severe visual impairment on the cortical organization and connectivity of primary visual cortex? Front Neuroanat 3:30. CrossRef Medline

Lau CG, Murthy VN (2012) Activity-dependent regulation of inhibition via GAD67. J Neurosci 32:8521–8531. CrossRef Medline

Laurie DJ, Wisden W, Seeburg PH (1992) The distribution of thirteen GABAA receptor subunit mRNAs in the rat brain. III. Embryonic and postnatal development. J Neurosci 12:4151–4172. Medline

Leysen I, Van der Gucht E, Eysel UT, Huybrechts R, Vandesande F, Arckens L (2004) Time-dependent changes in the expression of the MEF2 transcription factor family during topographic map reorganization in mammalian visual cortex. Eur J Neurosci 20:769–780. CrossRef Medline

Liguz-Lecznar M, Waleszczyk WJ, Zakrzewska R, Skangiel-Kramska J, Kossut M (2009) Associative pairing involving monocular stimulation selectively mobilizes a subclass of GABAergic interneurons in the mouse visual cortex. J Comp Neurol 516:482–492. CrossRef Medline

Maffei A, Fontanini A (2009) Network homeostasis: a matter of coordination. Curr Opin Neurobiol 19:168–173. CrossRef Medline

Markram H, Toledo-Rodriguez M, Wang Y, Gupta A, Silberberg G, Wu C (2004) Interneurons of the neocortical inhibitory system. Nat Rev Neurosci 5:793–807. CrossRef Medline

Massie A, Cnops L, Jacobs S, Van Damme K, Vandenbussche E, Eysel UT, Vandesande F, Arckens L (2003a) Glutamate levels and transport in cat (*Felis catus*) area 17 during cortical reorganization following binocular retinal lesions. J Neurochem 84:1387–1397. CrossRef Medline

Massie A, Cnops L, Smolders I, Van Damme K, Vandenbussche E, Vandesande F, Eysel UT, Arckens L (2003b) Extracellular GABA concentrations in area 17 of cat visual cortex during topographic map reorganization following binocular central retinal lesioning. Brain Res 976:100–108. CrossRef Medline

Mataga N, Fujishima S, Condie BG, Hensch TK (2001) Experience-dependent plasticity of mouse visual cortex in the absence of the neuronal activity-dependent marker egr1/zif268. J Neurosci 21:9724–9732. Medline

McCoy P, Norton TT, McMahon LL (2008) Layer 2/3 synapses in monoc-

ular and binocular regions of tree shrew visual cortex express mAChR-dependent long-term depression and long-term potentiation. J Neurophysiol 100:336–345. CrossRef Medline

Meredith MA (2002) On the neuronal basis for multisensory convergence: a brief overview. Brain Res Cogn Brain Res 14:31–40. CrossRef Medline

Micheva KD, Busse B, Weiler NC, O'Rourke N, Smith SJ (2010) Single-synapse analysis of a diverse synapse population: proteomic imaging methods and markers. Neuron 68:639–653. CrossRef Medline

Morishita H, Hensch TK (2008) Critical period revisited: impact on vision. Curr Opin Neurobiol 18:101–107. CrossRef Medline

Mrsic-Flogel TD, Hofer SB, Ohki K, Reid RC, Bonhoeffer T, Hübener M (2007) Homeostatic regulation of eye-specific responses in visual cortex during ocular dominance plasticity. Neuron 54:961–972. CrossRef Medline

Murphy KM, Beston BR, Boley PM, Jones DG (2005) Development of human visual cortex: a balance between excitatory and inhibitory plasticity mechanisms. Dev Psychobiol 46:209–221. CrossRef Medline

Nataraj K, Turrigiano G (2011) Regional and temporal specificity of intrinsic plasticity mechanisms in rodent primary visual cortex. J Neurosci 31:17932–17940. CrossRef Medline

Nusser Z, Sieghart W, Benke D, Fritschy JM, Somogyi P (1996) Differential synaptic localization of two major gamma-aminobutyric acid type A receptor alpha subunits on hippocampal pyramidal cells. Proc Natl Acad Sci U S A 93:11939–11944. CrossRef Medline

Nys J, Aerts J, Ytebrouck E, Vreysen S, Laeremans A, Arckens L (2014) The cross-modal aspect of mouse visual cortex plasticity induced by monocular enucleation is age dependent. J Comp Neurol 522:950–970. CrossRef Medline

Nys J, Scheyltjens I, Arckens L (2015) Visual system plasticity in mammals: the story of enucleation-induced vision loss. Front Syst Neurosci 9:60. CrossRef Medline

Okada M, Onodera K, Van Renterghem C, Sieghart W, Takahashi T (2000) Functional correlation of $GABA_A$ receptor alpha subunits expression with the properties of IPSCs in the developing thalamus. J Neurosci 20:2202–2208. Medline

Okaty BW, Miller MN, Sugino K, Hempel CM, Nelson SB (2009) Transcriptional and electrophysiological maturation of neocortical fast-spiking GABAergic interneurons. J Neurosci 29:7040–7052. CrossRef Medline

Olcese U, Iurilli G, Medini P (2013) Cellular and synaptic architecture of multisensory integration in the mouse neocortex. Neuron 79:579–593. CrossRef Medline

Pallas SL (2001) Intrinsic and extrinsic factors that shape neocortical specification. Trends Neurosci 24:417–423. CrossRef Medline

Paperna T, Malach R (1991) Patterns of sensory intermodality relationships in the cerebral cortex of the rat. J Comp Neurol 308:432–456. CrossRef Medline

Paulussen M, Van Brussel L, Arckens L (2011) Monocular enucleation profoundly reduces secretogranin II expression in adult mouse visual cortex. Neurochem Int 59:1082–1094. CrossRef Medline

Petroski RE, Pomeroy JE, Das R, Bowman H, Yang W, Chen AP, Foster AC (2006) Indiplon is a high-affinity positive allosteric modulator with selectivity for alpha1 subunit-containing GABAA receptors. J Pharmacol Exp Ther 317:369–377. CrossRef Medline

Petrus E, Isaiah A, Jones AP, Li D, Wang H, Lee HK, Kanold PO (2014) Crossmodal induction of thalamocortical potentiation leads to enhanced information processing in the auditory cortex. Neuron 81:664–673. CrossRef Medline

Pinto JG, Hornby KR, Jones DG, Murphy KM (2010) Developmental changes in GABAergic mechanisms in human visual cortex across the lifespan. Front Cell Neurosci 4:16. CrossRef Medline

Qu Y, Massie A, Van der Gucht E, Cnops L, Vandenbussche E, Eysel UT, Vandesande F, Arckens L (2003) Retinal lesions affect extracellular glutamate levels in sensory-deprived and remote non-deprived regions of cat area 17 as revealed by in vivo microdialysis. Brain Res 962:199–206. CrossRef Medline

Reetz A, Solimena M, Matteoli M, Folli F, Takei K, De Camilli P (1991) GABA and pancreatic beta-cells: colocalization of glutamic acid decarboxylase (GAD) and GABA with synaptic-like microvesicles suggests their role in GABA storage and secretion. EMBO J 10:1275–1284. Medline

Saffen DW, Cole AJ, Worley PF, Christy BA, Ryder K, Baraban JM (1988) Convulsant-induced increase in transcription factor messenger RNAs in rat brain. Proc Natl Acad Sci U S A 85:7795–7799. CrossRef Medline

Semyanov A, Walker MC, Kullmann DM, Silver RA (2004) Tonically active GABAA receptors: modulating gain and maintaining the tone. Trends Neurosci 27:262–269. CrossRef Medline

Soghomonian JJ, Martin DL (1998) Two isoforms of glutamate decarboxylase: why? Trends Pharmacol Sci 19:500–505. CrossRef Medline

Stehberg J, Dang PT, Frostig RD (2014) Unimodal primary sensory cortices are directly connected by long-range horizontal projections in the rat sensory cortex. Front Neuroanat 8:93. CrossRef Medline

Sullivan SK, Petroski RE, Verge G, Gross RS, Foster AC, Grigoriadis DE (2004) Characterization of the interaction of indiplon, a novel pyrazolopyrimidine sedative-hypnotic, with the GABAA receptor. J Pharmacol Exp Ther 311:537–546. CrossRef Medline

Syken J, Grandpre T, Kanold PO, Shatz CJ (2006) PirB restricts ocular-dominance plasticity in visual cortex. Science 313:1795–1800. CrossRef Medline

Tabuchi K, Blundell J, Etherton MR, Hammer RE, Liu X, Powell CM, Südhof TC (2007) A neuroligin-3 mutation implicated in autism increases inhibitory synaptic transmission in mice. Science 318:71–76. CrossRef Medline

Tagawa Y, Kanold PO, Majdan M, Shatz CJ (2005) Multiple periods of functional ocular dominance plasticity in mouse visual cortex. Nat Neurosci 8:380–388. CrossRef Medline

Toldi J, Farkas T, Völgyi B (1994) Neonatal enucleation induces cross-modal changes in the barrel cortex of rat. A behavioural and electrophysiological study. Neurosci Lett 167:1–4. CrossRef Medline

Toldi J, Fehér OO, Wolff JR (1996) Neuronal plasticity induced by neonatal monocular (and binocular) enucleation. Prog Neurobiol 48:191–218. CrossRef Medline

Trachtenberg JT, Trepel C, Stryker MP (2000) Rapid extragranular plasticity in the absence of thalamocortical plasticity in the developing primary visual cortex. Science 287:2029–2032. CrossRef Medline

Turrigiano GG, Leslie KR, Desai NS, Rutherford LC, Nelson SB (1998) Activity-dependent scaling of quantal amplitude in neocortical neurons. Nature 391:892–895. CrossRef Medline

van Brussel L, Gerits A, Arckens L (2009) Identification and localization of functional subdivisions in the visual cortex of the adult mouse. J Comp Neurol 514:107–116. CrossRef Medline

Van Brussel L, Gerits A, Arckens L (2011) Evidence for cross-modal plasticity in adult mouse visual cortex following monocular enucleation. Cereb Cortex 21:2133–2146. CrossRef Medline

Van Damme K, Massie A, Vandesande F, Arckens L (2003) Distribution of the AMPA2 glutamate receptor subunit in adult cat visual cortex. Brain Res 960:1–8. CrossRef Medline

Van der Gucht E, Hof PR, Van Brussel L, Burnat K, Arckens L (2007) Neurofilament protein and neuronal activity markers define regional architectonic parcellation in the mouse visual cortex. Cereb Cortex 17:2805–2819. CrossRef Medline

Vasconcelos N, Pantoja J, Belchior H, Caixeta FV, Faber J, Freire MA, Cota VR, de Macedo E, Laplagne DA, Gomes HM, Ribeiro S (2011) Cross-modal responses in the primary visual cortex encode complex objects and correlate with tactile discrimination. Proc Natl Acad Sci U S A 108:15408–15413. CrossRef Medline

Wagor E, Mangini NJ, Pearlman AL (1980) Retinotopic organization of striate and extrastriate visual cortex in the mouse. J Comp Neurol 193:187–202. CrossRef Medline

Wakabayashi K, Narisawa-Saito M, Iwakura Y, Arai T, Ikeda K, Takahashi H, Nawa H (1999) Phenotypic down-regulation of glutamate receptor subunit GluR1 in Alzheimer's disease. Neurobiol Aging 20:287–295. CrossRef Medline

Wei W, Zhang N, Peng Z, Houser CR, Mody I (2003) Perisynaptic localization of delta subunit-containing $GABA_A$ receptors and their activation by GABA spillover in the mouse dentate gyrus. J Neurosci 23:10650–10661. Medline

Wenner P (2011) Mechanisms of GABAergic homeostatic plasticity. Neural Plast 2011:489470. CrossRef Medline

Wisden W, Laurie DJ, Monyer H, Seeburg PH (1992) The distribution of 13 GABAA receptor subunit mRNAs in the rat brain. I. Telencephalon, diencephalon, mesencephalon. J Neurosci 12:1040–1062. Medline

Woolley DG, Laeremans A, Gantois I, Mantini D, Vermaercke B, Op de Beeck HP, Swinnen SP, Wenderoth N, Arckens L, D'Hooge R (2013) Homol-

ogous involvement of striatum and prefrontal cortex in rodent and human water maze learning. Proc Natl Acad Sci U S A 110:3131–3136. CrossRef Medline

Worley PF, Christy BA, Nakabeppu Y, Bhat RV, Cole AJ, Baraban JM (1991) Constitutive expression of zif268 in neocortex is regulated by synaptic activity. Proc Natl Acad Sci U S A 88:5106–5110. CrossRef Medline

Wu H, Jin Y, Buddhala C, Osterhaus G, Cohen E, Jin H, Wei J, Davis K, Obata K, Wu JY (2007) Role of glutamate decarboxylase (GAD) isoform, GAD65, in GABA synthesis and transport into synaptic vesicles—evidence from GAD65-knockout mice studies. Brain Res 1154:80–83. CrossRef Medline

Yagi F, Sakai M, Ikeda Y, Okutani F, Takahashi S, Fukata J (2001) Reorganization of the uncrossed visual pathways as revealed by Fos-like immunoreactivity in rats with neonatal monocular enucleation. Neurosci Lett 304:53–56. CrossRef Medline

Yoshitake K, Tsukano H, Tohmi M, Komagata S, Hishida R, Yagi T, Shibuki K (2013) Visual map shifts based on whisker-guided cues in the young mouse visual cortex. Cell Rep 5:1365–1374. CrossRef Medline

Zangenehpour S, Chaudhuri A (2002) Differential induction and decay curves of c-fos and zif268 revealed through dual activity maps. Mol Brain Res 109:221–225. CrossRef Medline

Zhang F, Halleux P, Arckens L, Vanduffel W, Van Brée L, Mailleux P, Vandesande F, Orban GA, Vanderhaeghen JJ (1994) Distribution of immediate early gene zif-268, c-fos, c-jun and jun-D mRNAs in the adult cat with special references to brain region related to vision. Neurosci Lett 176:137–141. CrossRef Medline